



doi:10.1016/S0016-7037(03)00161-3

Pb-Sr-He isotope and trace element geochemistry of the Cape Verde Archipelago

RÉGIS DOUCELANCE,^{1,2,*} STÉPHANE ESCRIG,¹ MANUEL MOREIRA,^{3,†} CLÉMENT GARIÉPY,² and MARK D. KURZ³¹Laboratoire de Géochimie et Cosmochimie (UMR 7579 CNRS), Institut de Physique du Globe de Paris, Université Denis Diderot Paris 7, 4 Place Jussieu, 75252 Paris cedex 05, France²GEOTOP-UQAM-McGILL, CP 8888, Succursale Centre-Ville, Montréal, QC H3C 3P8, Canada³Department of Marine Chemistry and Geochemistry, Woods Hole Oceanographic Institution, 360 Woods Hole Road, MS25, Woods Hole, MA 02543, USA

(Received September 13, 2002; revised 17 February 2003; accepted in revised form February 17, 2003)

Abstract—New lead, strontium and helium isotopic data, together with trace element concentrations, have been determined for basalts from the Cape Verde archipelago (Central Atlantic). Isotopic and chemical variations are observed at the scale of the archipelago and lead to the definition of two distinct groupings, in keeping with earlier studies. The Northern Islands (Santo Antão, São Vicente, São Nicolau and Sal) present Pb isotopic compositions below the Northern Hemisphere Reference Line (NHRL) (cf. Hart, 1984), unradiogenic Sr and relatively primitive $^4\text{He}/^3\text{He}$ ratios. In contrast, the Southern Islands (Fogo and Santiago) display Pb isotopes above the NHRL, moderately radiogenic Sr and MORB-like helium signatures. We propose that the dichotomy between the Northern and Southern Islands results from the presence of three isotopically distinct components in the source of the Cape Verde basalts: (1) recycled ~ 1.6 -Ga oceanic crust (high $^{206}\text{Pb}/^{204}\text{Pb}$, low $^{87}\text{Sr}/^{86}\text{Sr}$ and high $^4\text{He}/^3\text{He}$); (2) lower mantle material (high ^3He); and (3) subcontinental lithosphere (low $^{206}\text{Pb}/^{204}\text{Pb}$, high $^{87}\text{Sr}/^{86}\text{Sr}$ and moderately radiogenic $^4\text{He}/^3\text{He}$ ratios). The signature of the Northern Islands reflects mixing between recycled oceanic crust and lower mantle, to which small proportions of entrained depleted material from the local upper mantle are added. Basalts from the Southern Islands, however, require the addition of an enriched component thought to be subcontinental lithospheric material instead of depleted mantle. The subcontinental lithosphere may stem from delamination and subsequent incorporation into the Cape Verde plume, or may be remnant from delamination just before the opening of the Central Atlantic. Basalts from São Nicolau reflect the interaction with an additional component, which is identified as oceanic crustal material. Copyright © 2003 Elsevier Ltd

1. INTRODUCTION

Isotopic variations in ocean island basalts (OIB) are now commonly interpreted as resulting from the mixtures between various components. These mixtures have several end-members (Zindler et al., 1982; Allègre and Turcotte, 1985; White, 1985; Zindler and Hart, 1986a; Allègre et al., 1986/1987), termed HIMU (for high μ), EMI and EMII (for Enriched Mantle I and II) and DMM (for Depleted MORB Mantle) by Zindler and Hart (1986a). However, the exact nature of these end-members is still debated. The HIMU end-member is generally thought to represent recycling of subduction of ancient and altered oceanic crust (Hofmann and White, 1982; Allègre, 1987; Weaver, 1991; Chauvel et al., 1992; Thirlwall, 1997). Intermediate, HIMU-like signatures measured in some oceanic basalts (also termed “young” HIMU) are either explained by the mixture between DMM and HIMU material or by the presence of relatively young recycled oceanic crust (Thirlwall, 1997). The characteristics of EMI and EMII have been associated with old pelagic and/or terrigenous sediments, recycled with, or without, oceanic crust (Allègre, 1987; Weaver, 1991;

Chauvel et al., 1992) or related, in the case of EMI, to subcontinental lithospheric mantle material (Cohen and O’Nions, 1982; McKenzie and O’Nions, 1983). It has also been proposed that both HIMU and EM end-members result from intra-mantle metasomatic processes (Vollmer, 1983; Hart, 1988; Hawkesworth et al., 1990).

In comparison, rare gas systematics, notably He isotope signatures, provide good evidence for the involvement of lower mantle material in some OIB sources. Indeed, mid-ocean ridge basalts (MORB) display a quite constant $^4\text{He}/^3\text{He}$ ratio of $88,000 \pm 5000$ ($R/R_A = 8 \pm 1$; R/R_A is the $^3\text{He}/^4\text{He}$ ratio normalized to the atmospheric value of 1.384×10^{-6}), corresponding to the mean value of the degassed upper mantle (Kurz et al., 1982; Allègre et al., 1995), whereas higher R/R_A ratios measured in OIB (up to ~ 43 in Icelandic lavas, cf. Breddam and Kurz, 2001) reflect a relatively undegassed reservoir thought to be the lower mantle (Kurz et al., 1982). Lower R/R_A measured in some EM- and HIMU-OIB are, however, a source of controversy. They are either attributed to the recycling of oceanic crust and/or sediments into the mantle, characterized by high $(\text{U} + \text{Th})/^3\text{He}$ ratios, which were stored for some time at the 670-km boundary layer (Kurz et al., 1982; Graham et al., 1992; Hanyu and Kaneoka, 1997; Moreira et al., 1999), or to magma chamber contamination processes (Condomines et al., 1983; Zindler and Hart, 1986b; Hilton et al., 1995).

The study of different OIB archipelagos around the world is very useful in clarifying such problems. The first detailed geochemical study of the Cape Verde was that of Gerlach et al. (1988) who determined trace element concentrations and Sr-

* Author to whom correspondence should be addressed, at Laboratoire Magmas et Volcans, Université Blaise Pascal, CNRS (UMR 6524), Observatoire de Physique du Globe de Clermont-Ferrand, 5 Rue Kessler, 63038, Clermont-Ferrand cedex, France (doucelance@opgc.univ-bpclermont.fr).

† Present address: Laboratoire de Géochimie et Cosmochimie (UMR 7579 CNRS), Institut de Physique du Globe de Paris, Université Denis Diderot Paris 7, 4 Place Jussieu, 75252 Paris cedex 05, France.

Nd-Pb isotopic compositions of lavas from five islands. They pointed out differences between the Southern and Northern Islands, and interpreted them as reflecting the presence of three isotopically distinct end-members: (1) Depleted MORB Mantle (DMM); (2) a HIMU-like end-member; and (3) an EMI-like end-member. These results have been confirmed by the subsequent study of Davies et al. (1989) who presented a comparison between the Azores and Cape Verde archipelagos. Concerning the geodynamic context of lava generation, Gerlach et al. (1988) presented two different models. In the first, the EMI-like end-member is located at the base of the oceanic lithosphere and only contributes to magmatism in the Southern Islands; the HIMU-like end-member, supplied by the plume and possibly supplemented by “entrained” DMM material, explains the isotopic compositions of the Northern Islands. In the second model, the Cape Verde plume displays EMI-like characteristics and the HIMU end-member is present in the upper mantle as pyroxene-rich recycled oceanic crust, in a fashion similar to the marble cake mantle of Allègre and Turcotte (1986). The absence of EMI contributions in the Northern Islands would thus result from a smaller degree of partial melting.

Kokfelt et al. (1998) suggested an alternative model in which both the EMI- and HIMU-like end-members reside in the oceanic lithosphere above the non-melting Cape Verde mantle plume. Based on Sr, Nd and Pb isotopic compositions, U/Th measurements and trace element data, these authors proposed that: (1) the HIMU-like end-member corresponds to a so-called “young HIMU” component resulting from metasomatism by carbonatitic fluids of the oceanic crust associated with the degassing of the mantle just before the opening of the Atlantic ocean; and (2) the EMI end-member is related to delaminated subcontinental lithosphere. Jørgensen and Holm (2002), however, proposed the existence of two separate HIMU-like end-members within the Cape Verde plume to explain the isotopic signature of basalts and carbonatites sampled on São Vicente island.

Finally, Christensen et al. (2001) presented the first rare gas results (He and Ar) as well as Pb isotopic results for the two youngest islands of the archipelago: Fogo and Santo Antão. They confirmed the presence of a “young HIMU” end-member in the source of the Cape Verde magmas, but also argued for the involvement of lower mantle material in the Northern Islands to explain the moderately primitive He ratios of Santo Antão basalts ($^4\text{He}/^3\text{He} \sim 50,000$). Due to the small number of He and Pb data available from Fogo, they did not draw any conclusions in favour of such a lower mantle contribution in the Southern Islands, nor about the EMI-like end-member previously identified by Gerlach et al. (1988), Davies et al. (1989) and Kokfelt et al. (1998).

In this study we present new Pb, Sr and He analyses, together with trace element concentrations, for five islands of the Cape Verde Archipelago: Fogo, Santiago, São Vicente, São Nicolau and Sal (Fig. 1). Using time-integrated models, we calculate the isotopic composition for Pb, Sr and He of recycled oceanic crust, delaminated subcontinental lithosphere and lower mantle materials. We then consider the presence of these three components in the source of the Cape Verde basalts and discuss the geodynamic implications.

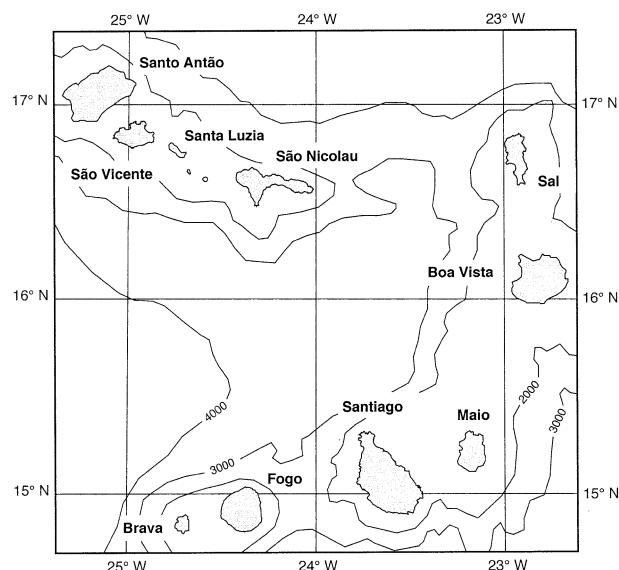


Fig. 1. Location map and sea-floor bathymetry of the Cape Verde archipelago, modified after Gerlach et al. (1988).

2. GEOGRAPHIC LOCATION, TECTONIC SETTING AND GEOLOGICAL DESCRIPTION

The Cape Verde Islands are located ~500 km to the west of Senegal, between latitudes 15 and 17°N. The archipelago is composed of 10 principal islands, which can be divided into two groups: (1) the Southern Islands of Brava, Fogo, Santiago and Maio; and (2) the Northern Islands of Santo Antão, São Vicente, Santa Luzia and São Nicolau, extending to the east with Sal and Boa Vista (Fig. 1). In the two groups, the alignment of islands is thought to be controlled by: (1) a deep structure (possibly an old oceanic ridge) present in this part of Atlantic since the Mesozoic (Klerkx and De Paepe, 1971); and (2) a transverse fracture zone (Le Pichon and Fox, 1971). The Cape Verde archipelago constitutes one of the highest oceanic plateaux, with an average depth of 2 km above the oceanic floor. Anomalous heat flow and geoid data cannot be explained by reheating of the oceanic lithosphere alone, implying the presence of a thermal plume (Courtney and White, 1986). Although the archipelago is located quite close to the African continent, its position relative to the continental slope does not suggest the presence of continental crust under the Cape Verde Islands (Klerkx et al., 1974).

The oldest submarine formations formed in the Jurassic (Klerkx et al., 1974). For exposed volcanic rocks on the islands, magmatic activity probably started in the Miocene for the youngest (Brava, Fogo, Santo Antão and São Vicente), and between the initial- and middle-parts of the Cenozoic for the others (Gerlach et al., 1988). Currently, volcanism is restricted to Brava and Fogo with the most recent eruption of the Fogo volcano occurring on April 3, 1995. There is a regional ageing of the Southern Islands from the west (Brava) to the east (Maio), consistent with the movement of the oceanic plate toward the northeast. However, due to its location near the pole of rotation of the African plate, the Cape Verde archipelago appears to have remained quite stationary relative to a fixed hotspot frame of reference (Duncan, 1980) for the last 20 Ma,

with a relative speed of ~ 12 mm/yr (Courtney and White, 1986).

Exposed magmatic units on all islands of the archipelago have a volcanic origin, except for rare, discrete carbonatite intrusives (Allègre et al., 1971; Hoernle et al., 2002). The lavas define a petrographic series ranging from nephelinites to phonolites (De Paepe et al., 1974; Klerkx et al., 1974). Some important calcareous deposits are also present on Sal, Boa Vista and Maio (Matos Alves et al., 1979; Gerlach et al., 1988). For this study, we analyzed lavas from Fogo, Santiago, São Vicente, São Nicolau and Sal which were collected in February 1998. Sample locations are illustrated in Figure 2.

3. ANALYTICAL PROCEDURE

Lead chemical separation was done using ~ 1 g of whole-rock powder, following the procedure of Manhès et al. (1978), in a clean room under controlled atmosphere. Total Pb blanks are < 0.5 ng and show a common isotopic composition, making corrections in all cases negligible with respect to sample Pb contents. Lead isotopic ratios were measured on a VG354 thermal ionization mass spectrometer used in peak jumping mode; the instrument was calibrated against the NIST SRM981 standard (Catanzaro et al., 1968) yielding a statistical mass bias factor of $0.1 \pm 0.03\%$ per mass unit difference in the isotopic ratios. Additional values were obtained at the GEOTOP laboratory (Montréal, Canada) using a Micromass IsoProbe MC-ICP-MS operated in static mode. Chemical separation was performed with $10 \mu\text{L}$ column volume of AG1X8 resin (loading and washing in 0.8N HBr , elution in 6.2N HCl) on ~ 100 mg of the powdered samples; blanks were in the range of 100 to 150 pg and negligible. Tail corrections on the IsoProbe instrument were based on abundance sensitivity measurements of separate ^{204}Pb and ^{208}Pb isotope solutions instead of half-mass zeroes (Thirlwall, 2001, 2002). Mass fractionation was corrected for by using the Tl doping technique and an exponential law, assuming identical fractionation factors for both Pb and Tl. External reproducibility between the Pb measurements done on the TIMS and the MC-ICP-MS instruments was corrected for by adjusting the $^{205}\text{Tl}/^{203}\text{Tl}$ ratio to 2.38884, thus yielding a mean of 0.91464 for the $^{207}\text{Pb}/^{206}\text{Pb}$ ratio of NIST SRM981 (Catanzaro et al., 1968). Total reproducibility is better than 0.04% (2σ) per amu; it can be evaluated using samples F-02 (A and B) and F-15 (A and B) which were measured on both instruments. Samples F-08b (A and B), F-11 (A and B) and F-12 (A, B, and C) are duplicates of the total procedure developed in Montréal.

Strontium isotopic measurements were done also using the VG354 mass spectrometer after chemical separation using a Sr Spec Column (Pin and Bassin, 1992). Sr blank for the complete procedure was between 30 and 80 pg. Isotopic measurements were mass-fractionation-corrected using $^{86}\text{Sr}/^{88}\text{Sr} = 0.1194$ and normalized to $^{87}\text{Sr}/^{86}\text{Sr} = 0.71025$ for the NIST SRM987 standard. Total reproducibility, tested on replicate analyses of SRM987, was better than 0.002% (2σ). Some leaching experiments have also been performed on three basalts from São Vicente, by using hot 6N HCl over a period of 8 h (Dupré et al., 1982).

Helium analyses were performed on millimeter-sized olivine and pyroxene phenocrysts separated from fresh lavas. Measurements were done by crushing these materials, to avoid possible

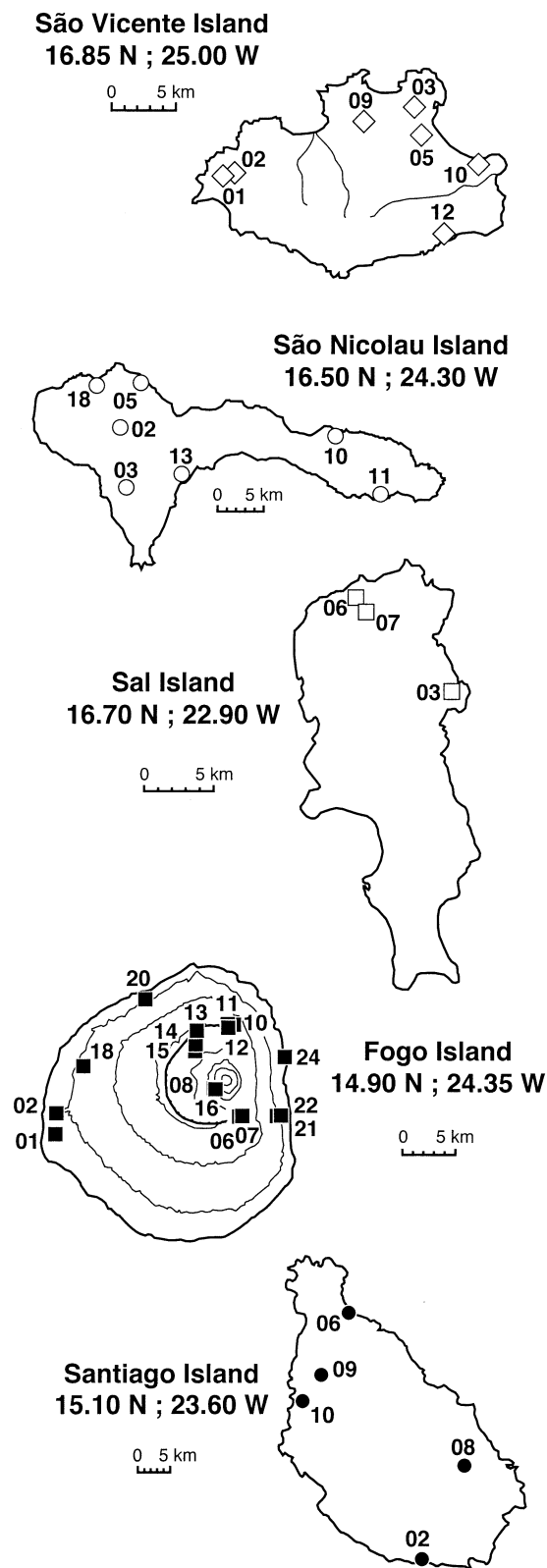


Fig. 2. Fogo, Santiago, São Vicente, São Nicolau and Sal island sampling maps.

Table 1. Major (%) and trace element (ppm) concentrations of samples from Cape Verde.

	Fogo (F-)						Santiago (ST-)				
	02	07	08	15	20	24	02	06	08	09	10
SiO ₂	41.59	42.24	42.47	42.14	40.65	41.42	42.96	38.08	42.91	39.45	41.66
Al ₂ O ₃	14.88	15.32	15.59	15.71	14.53	13.31	12.92	10.22	11.80	14.75	15.49
Fe ₂ O ₃	14.19	13.31	13.24	13.06	14.07	14.18	12.39	12.49	12.38	12.36	11.02
MnO	0.18	0.20	0.20	0.21	0.20	0.20	0.17	0.18	0.17	0.23	0.17
MgO	7.15	6.49	6.17	5.81	6.50	9.21	10.40	13.19	10.71	6.25	5.82
CaO	11.07	12.02	11.94	11.60	12.81	12.81	12.89	14.54	12.74	13.05	11.19
Na ₂ O	4.41	3.75	3.89	4.00	3.61	3.08	2.82	3.16	1.89	3.34	2.67
K ₂ O	2.18	2.60	2.74	2.77	2.39	1.92	1.23	2.08	1.34	1.78	2.91
TiO ₂	4.07	3.74	3.80	3.65	4.40	3.53	2.66	3.59	3.20	3.50	3.91
P ₂ O ₅	0.60	0.82	0.84	0.91	0.70	0.74	0.58	0.72	0.48	1.20	0.92
Total	100.32	100.49	100.88	99.86	99.86	100.40	99.02	98.25	97.62	95.91	95.76
L.O.I.	—	—	—	—	—	—	1.17	1.59	2.32	3.92	4.40
Rb	63	56	60	61	49	43	24	43	33	58	59
Ba	795	802	849	771	747	634	963	700	561	986	844
Th	4.5	5.1	5.7	5.6	4.1	4.0	5.0	6.3	4.6	15.4	8.5
U	0.97	1.05	1.19	1.25	0.96	0.88	1.14	1.36	0.92	4.71	2.06
Nb	83	84	90	89	77	67	69	81	62	165	112
Ta	6.57	6.38	7.04	7.20	6.30	5.24	4.70	5.64	4.39	12.10	9.00
La	45	56	59	57	49	47	51	58	45	132	87
Ce	98	124	131	124	110	100	102	117	89	252	175
Pr	11.6	14.8	15.7	15.4	14.0	13.1	12.1	14.0	11.1	29.3	20.7
Nd	47	57	63	64	58	54	48	58	44	115	81
Sr	929	1041	1066	1104	1014	893	930	824	910	2064	1652
Sm	9.1	10.8	11.4	11.3	10.8	10.0	8.7	10.3	8.9	19.4	14.0
Zr	330	338	357	357	356	281	236	326	285	502	437
Eu	2.84	3.41	3.70	3.64	3.70	3.25	2.93	3.10	2.61	5.72	4.37
Gd	6.74	8.78	9.06	9.41	8.78	8.18	6.95	7.17	6.47	14.10	11.00
Tb	0.98	1.22	1.33	1.25	1.25	1.09	0.98	1.05	0.97	1.99	1.49
Dy	5.00	6.12	6.49	6.33	6.47	5.70	4.81	5.51	4.86	9.81	7.63
Ho	0.868	1.020	1.030	1.120	1.060	0.973	0.820	0.888	0.884	1.670	1.350
Er	2.05	2.59	2.57	2.64	2.45	2.19	2.00	2.06	2.01	3.85	2.98
Tm	0.271	0.294	0.314	0.339	0.358	0.300	0.230	0.239	0.266	0.530	0.420
Y	23.4	29.1	29.9	31.0	29.5	27.2	22.1	24.6	25.0	44.5	34.7
Yb	1.81	2.17	2.12	2.27	1.96	1.80	1.47	1.35	1.43	2.88	2.39
Lu	0.251	0.290	0.310	0.308	0.284	0.256	0.230	0.233	0.233	0.453	0.307
Co	47	43	40	41	47	54	52	62	61	37	35
Ni	83	50	42	34	43	113	211	313	274	34	39

in situ radiogenic decay products or cosmogenic ³He and to obtain the volcanic helium gas trapped in inclusions (Kurz et al., 1982; Kurz, 1986). Some samples were also melted under vacuum conditions to release the gases located in the matrix and evaluate the content of radiogenic and cosmogenic helium. Measurements were done in the Woods Hole Oceanographic Institution with an automated mass spectrometer; the total blank is typically 3 to 5 × 10⁻¹¹ cm³ STP (Kurz et al., 1996).

Whole-rock major- and trace-element results were obtained from the Service d'Analyse des Roches et des Minéraux (SARM) at the Centre de Recherches Pétrographiques et Géochimiques (CRPG/Nancy). Major- and trace-element contents were determined by ICP-AES and ICP-MS, respectively, after alkaline melting with lithium borate and nitric acid dissolution. International standards as well as analytical procedures used in the CRPG laboratory at Nancy can be downloaded from the Web site at <http://www.cprg.cnrs-nancy.fr/SARM/index.html>.

4. MAJOR AND TRACE ELEMENT VARIATIONS

All samples have SiO₂ contents <45% (Table 1); they are mafic lavas corresponding to nephelinites, picro-basalts, basan-

ites and tephrites. Such an abundance of mafic rocks was already noted by Klerkx et al. (1974) and Gerlach et al. (1988). The major element abundances do not define any significant variations as the samples are not strongly differentiated. However, the MgO contents are regionally lower for samples collected on the Southern Islands (5.81–13.19, mean = 7.97, compared to 10.10–19.97, mean = 13.14, for the Northern Islands) and, in a general way, samples from the Southern Islands display a more alkaline character than those from the Northern Islands.

The dichotomy suggested by major element abundances can be shown more clearly when considering trace elements. For example, Figure 3 presents a Th/Nb vs. Th/Tb plot where samples from the Northern and Southern Islands define two different trends. These can be explained by the melting of two distinct sources for Th, Nb and Tb (Joron and Treuil, 1989). Modeling based on São Nicolau and São Vicente samples, for which crystal fractionation is most probably only minimal (high and relatively constant Ni and Cr contents; Table 1), shows that variations of the Th/Nb and Th/Tb ratios can be reproduced by the batch melting of a harzburgite containing amphibole, phlogopite and ilmenite (Fig. 3; Table 2). Mineral

Table 1. (Continued)

São Vicente (SV-)							São Nicolau (SN-)							Sal (S-)		
01	02	03	05	09	10	12	02	03	05	10	11	13	18	03	06	07
44.33	43.07	44.47	40.60	38.54	38.84	43.28	41.70	42.52	40.45	39.97	41.89	44.47	44.47	35.67	38.25	38.89
13.23	11.27	13.34	10.59	11.24	11.34	8.38	11.88	13.20	12.28	11.93	12.47	13.17	13.87	10.93	9.59	8.25
12.12	12.59	12.55	13.23	13.27	13.09	13.52	13.36	13.05	12.95	12.90	12.85	11.59	12.55	12.20	12.92	13.37
0.17	0.17	0.18	0.17	0.17	0.18	0.17	0.20	0.18	0.19	0.21	0.19	0.18	0.17	0.20	0.19	0.19
10.10	11.33	10.77	15.19	12.05	12.69	18.96	14.20	10.87	12.62	12.48	12.13	10.40	10.16	12.90	16.52	19.97
12.24	13.80	11.92	12.12	12.89	14.17	9.71	11.50	12.41	13.65	14.02	12.83	12.27	10.81	16.42	13.37	12.48
2.09	2.05	3.27	2.75	2.93	2.75	1.19	3.67	1.98	3.93	3.63	3.29	3.01	2.66	3.07	2.59	1.80
1.10	1.01	1.25	0.60	0.35	1.25	0.63	0.56	0.73	0.76	1.03	1.06	1.13	1.03	0.93	1.34	1.04
3.11	3.42	2.69	3.28	4.42	3.69	2.25	2.77	3.47	3.11	2.85	2.74	2.71	2.82	3.34	3.40	3.31
0.43	0.41	0.41	0.53	0.65	0.61	0.30	0.53	0.41	0.74	0.79	0.60	0.40	0.45	1.44	0.68	0.48
98.92	99.12	100.85	99.06	96.51	98.61	98.39	100.37	98.82	100.68	99.79	100.05	99.33	98.99	97.10	98.85	99.76
1.35	0.90	—	1.20	3.59	1.51	1.65	—	1.21	—	0.18	—	0.26	1.05	2.30	0.49	0.32
25	20	23	7	27	23	15	28	18	14	18	25	30	21	33	31	25
331	264	377	392	591	517	204	423	324	494	498	534	355	392	929	514	352
4.7	3.0	2.9	3.7	6.0	4.5	2.3	4.0	2.9	6.3	7.8	4.1	4.4	3.7	12.2	6.2	3.3
1.08	0.72	0.52	0.82	1.03	0.99	0.5	0.8	0.67	1.16	1.54	1.09	0.93	0.85	2.95	1.31	0.75
49	40	44	47	73	62	28	54	48	65	74	54	48	51	89	67	47
3.56	3.05	3.45	3.57	5.12	4.46	2.01	3.83	3.31	4.21	5.15	3.59	3.46	3.80	6.15	4.81	3.40
36	29	25	36	54	43	22	35	28	51	58	41	33	33	92	52	36
76	66	55	76	112	90	48	71	64	99	114	85	67	70	181	108	77
9.0	8.3	6.7	9.0	12.6	10.7	5.7	8.4	7.8	11.8	13.2	10.1	7.9	8.3	21.2	13.4	9.7
36	35	29	37	54	44	24	35	33	48	54	39	31	33	80	51	39
611	555	590	659	1026	786	348	611	653	866	876	775	544	614	1515	902	643
7.6	7.2	5.8	7.1	10.0	8.3	5.0	6.8	6.6	8.4	9.6	7.8	6.7	7.1	14.8	10.2	8.0
215	207	173	206	270	219	142	197	234	228	221	219	229	215	301	236	216
2.41	2.30	2.04	2.22	3.02	2.71	1.64	2.25	2.09	2.86	3.22	2.64	2.28	2.35	4.43	3.00	2.53
6.08	6.57	5.64	5.69	8.39	6.97	4.49	6.02	5.84	7.84	8.52	6.91	5.97	6.00	11.10	7.74	6.65
0.97	0.90	0.90	0.85	1.11	0.97	0.64	0.91	0.84	1.04	1.17	0.92	0.87	0.91	1.44	1.14	0.89
4.84	4.56	4.34	4.22	5.50	4.99	3.30	4.55	4.66	5.53	6.16	5.26	4.84	5.06	7.56	5.57	4.32
0.886	0.848	0.802	0.755	1.000	0.808	0.604	0.852	0.911	0.959	1.145	0.977	0.851	1.020	1.180	0.897	0.741
2.19	1.85	2.08	1.87	2.21	1.90	1.37	2.09	2.13	2.21	2.56	2.24	2.11	2.33	3.14	2.06	1.57
0.315	0.275	0.286	0.243	0.291	0.256	0.228	0.301	0.298	0.299	0.353	0.291	0.333	0.370	0.346	0.269	0.203
25.4	23.3	22.6	20.8	26.0	23.3	16.3	24.6	26.1	28.9	31.6	28.1	25.3	26.3	35.5	25.4	19.7
1.90	1.68	1.57	1.37	1.66	1.40	1.24	1.78	1.92	1.80	2.18	1.85	2.05	2.17	2.48	1.67	1.31
0.273	0.227	0.252	0.238	0.238	0.206	0.197	0.264	0.298	0.295	0.315	0.296	0.283	0.325	0.323	0.245	0.170
53	62	57	70	61	60	83	67	59	62	60	60	51	52	58	72	78
205	214	216	454	252	282	553	349	163	257	245	261	211	221	232	466	611

proportions that best fit the evolution of Th/Nb and Th/Tb ratios measured in samples from the Northern Islands are ol:opx:cp:gt:amp:phlog:ilm = 77:16:1.5:3:0.25:0.75:1.5, for Th, Nb and Tb source contents of 0.09, 2.2 and 0.065 ppm, respectively, close to the reference Bulk Silicate Earth (McDonough and Sun, 1995). Class and Goldstein (1997) have developed the concept of an enrichment factor for trace elements. It corresponds to the concentration ratio, for a given element, between the sample with the lowest extent of partial melting and the sample with the highest one, in a series of cogenetic samples. Such enrichment factors were determined for the São Nicolau lavas: samples corresponding to the highest and lowest partial melting rate were chosen on the basis of Th vs. Nb contents. Figure 4 compares the enrichment factors thus calculated for São Nicolau with model values determined by Class and Goldstein (1997) for a harzburgite with amphibole, phlogopite and ilmenite. The overall agreement of factors for São Nicolau with those of Class and Goldstein (1997), as well as the modeling presented in Figure 3, suggest that basalts from the Northern and Southern Islands may result from the melting of two distinct sources containing amphibole and phlogopite. This is comparable with the results of Gerlach et al. (1988) who

interpreted positive trends between Rb and K abundances and K_2O/TiO_2 ratios in Cape Verde samples as reflecting phlogopite melting. The stability domain of such phases requires that melting occurred partly within the oceanic lithosphere.

Extended trace element patterns for the Fogo and Santiago samples (Figs. 5a and 5b) are similar to the EMI pattern defined by the mean composition of Tristan da Cunha volcanics (Le Roex et al., 1990; Cliff et al., 1991). In contrast, the Northern Island basalts display trace element enrichment with respect to primitive mantle (Figs. 5c–5e), similar to average Mangaia lavas (HIMU-like, cf. Woodhead, 1996) in Polynesia. These data are consistent with previous results and models (Gerlach et al., 1988; Davies et al., 1989) which showed the involvement of both EMI- and HIMU-like end-members in the source of the Cape Verde basalts. The low, but quite systematic, depletion which is observed for K relative to the lower mantle can be explained by the presence of a K-rich phase such as phlogopite in the source of the Cape Verde samples (Dupuy et al., 1988). However, Woodhead (1996) noted such a depletion was a common feature of ocean island basalts, and he interpreted this result as a graphic artefact due to the value of K chosen for normalization.

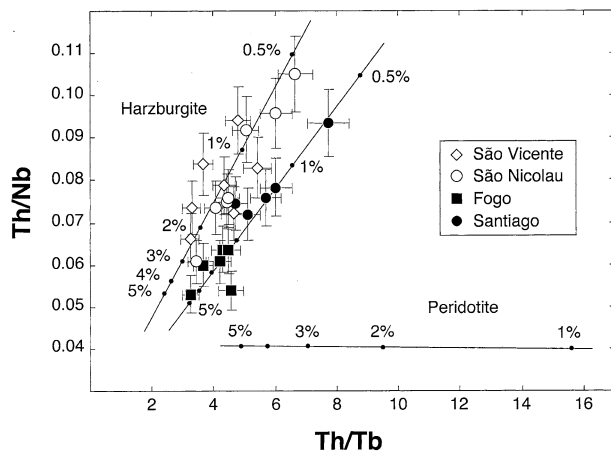


Fig. 3. Th/Nb vs. Th/Tb diagram for Cape Verde basalts in this study. Open symbols = Northern Islands; filled symbols = Southern Islands. Trace element data for São Vicente and São Nicolau samples are modeled by the batch melting of a harzburgite, containing amphibole, phlogopite and ilmenite in the proportion ol:opx:cp:gt:amp:phlog:ilm = 77:16:1.5:3:1:1:0.5 with Th, Nb and Tb source concentrations of 0.09, 2.2 and 0.065 ppm, respectively. The expected trend for a peridotite (ol:opx:cp:gt = 55:25:11:9) is also shown for comparison. The Th, Nb and Tb contents of the reference Bulk Silicate Earth are 0.0795, 0.658 and 0.099 ppm, respectively (McDonough and Sun, 1995). Fogo and Santiago results can be modeled either using the same mineralogy, but different source concentrations, or similar Th, Nb and Tb contents, but variable garnet, amphibole and ilmenite proportions.

5. LEAD-STRONTIUM-HELIUM ISOTOPE VARIATIONS

The variation ranges in Pb and Sr isotopic composition determined here (Table 3; Fig. 6) are of the same magnitude as those previously determined by Gerlach et al. (1988), Davies et al. (1989), Kokfelt et al. (1998), Christensen et al. (2001) and Jørgensen and Holm (2002). In parallel with the trace element signatures, the isotopic variations are related to the geographical position of the samples within the archipelago. Samples from the Southern Islands all have Pb isotopic compositions ($^{206}\text{Pb}/^{204}\text{Pb} = 18.883\text{--}19.398$; $^{207}\text{Pb}/^{204}\text{Pb} = 15.530\text{--}15.580$; and $^{208}\text{Pb}/^{204}\text{Pb} = 38.701\text{--}39.190$) plotting above the NHRL (Hart, 1984), for $^{87}\text{Sr}/^{86}\text{Sr}$ ratios in the range of 0.70349 to 0.70379. In contrast, the samples from the Northern Islands all yield Pb isotope ratios plotting below the NHRL ($^{206}\text{Pb}/^{204}\text{Pb} = 19.187\text{--}19.692$; $^{207}\text{Pb}/^{204}\text{Pb} = 15.564\text{--}15.619$; and $^{208}\text{Pb}/^{204}\text{Pb} = 38.763\text{--}39.401$) and $^{87}\text{Sr}/^{86}\text{Sr}$ ratios lower than the former, ranging from 0.70299 to 0.70336. Note that the São Nicolau samples appear to define a distinct alignment in the

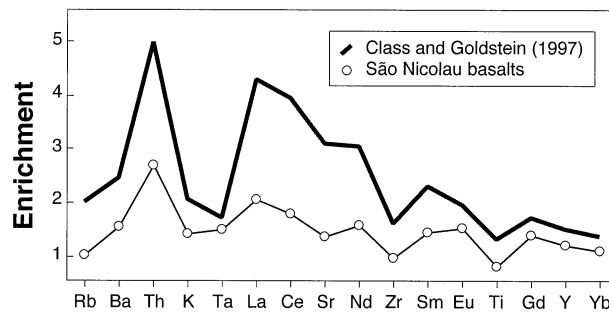


Fig. 4. Comparison between the enrichment factors of Class and Goldstein (1997) for a harzburgite with amphibole, phlogopite and ilmenite and values determined from São Nicolau basalts (see text for details).

$^{208}\text{Pb}/^{204}\text{Pb}$ (Fig. 6a) and $^{87}\text{Sr}/^{86}\text{Sr}$ (Fig. 6c) vs. $^{206}\text{Pb}/^{204}\text{Pb}$ diagrams. This may also be the case for the three basalt samples from Sal, but there are insufficient samples to confirm this trend. Lastly, leaching experiments that have been performed on three São Vicente samples do not show significant variations between residues and bulk samples (Table 3).

Helium concentrations obtained from crushing experiments (Table 4; Fig. 7a) range from $0.6 \times 10^{-9} \text{ cm}^3 \text{ STP/g}$ in olivines from sample SV-05 (São Vicente) to $5.12 \times 10^{-8} \text{ cm}^3 \text{ STP/g}$ in olivines from sample F-07 (Fogo). $^4\text{He}/^3\text{He}$ isotopic ratios vary from 45,928 ($R/R_A = 15.73$) to 522,824 ($R/R_A = 1.38$) in SN-10 (São Nicolau) and ST-09 (Santiago) samples, respectively. Blank levels were significantly higher in Santiago samples compared to other islands (Table 4) and correspond to olivines and pyroxenes which yielded the most radiogenic He values (e.g., ST-06 and ST-09). The helium concentration obtained from the melting experiment completed after crushing of CPXs from sample ST-09 is $15.28 \times 10^{-8} \text{ cm}^3 \text{ STP/g}$; the $^4\text{He}/^3\text{He}$ ratio is $4,128,819 \pm 117,966$ ($R/R_A = 0.18 \pm 0.01$), much more radiogenic than that of the crushed aliquot (Table 4). This strongly suggests in situ production of radiogenic ^4He , thus this sample probably does not reflect the isotopic composition of its magma source. The “re-crush” experiment carried out on sample ST-06, which initially had a radiogenic $^4\text{He}/^3\text{He}$ value of $185,505 \pm 38,054$ ($R/R_A = 3.9 \pm 0.8$), yielded a R/R_A value of 7.66 ± 2.77 (Table 4) which is consistent with other values determined for Santiago samples. However, the “melting” after crushing experiment carried out on olivines from this sample indicates the presence of cosmogenic ^3He (cf. left-hand portion of Fig. 7b) with a $^4\text{He}/^3\text{He}$ ratio of $24,741 \pm 231$ ($R/R_A = 29.20 \pm 0.27$). Figures 7c and 7d present replicates of crushing experiments for two samples (F-13 from Fogo and

Table 2. Partition coefficients.

	Olivine	OPX	CPX	Garnet	Amphibole	Phlogopite	Ilmenite
Th	0.00001	0.00003	0.03	0.0015	0.5	0.0014	0
Nb	0.0001	0.003	0.005	0.02	0.8	1.00	0.8
Tb	0.0028	0.012	0.57	0.705	0.635	0.03	0.14

D^{Th} for olivine and OPX: Beattie (1993a); D^{Th} (garnet): Beattie (1993b); D^{Th} (phlogopite): La Tourette et al. (1995); D^{Nb} (olivine and OPX): Kelemen et al. (1993); D^{Tb} (olivine): Beattie (1993a), D^{X} (ilmenite): Paster et al. (1974) except D^{Nb} : Irving (1978). All other partition coefficients can be found in Rollinson (1993), except D^{Th} (Olivine, OPX, amphibole and phlogopite) which were determined by linear interpolation with adjacent REE.

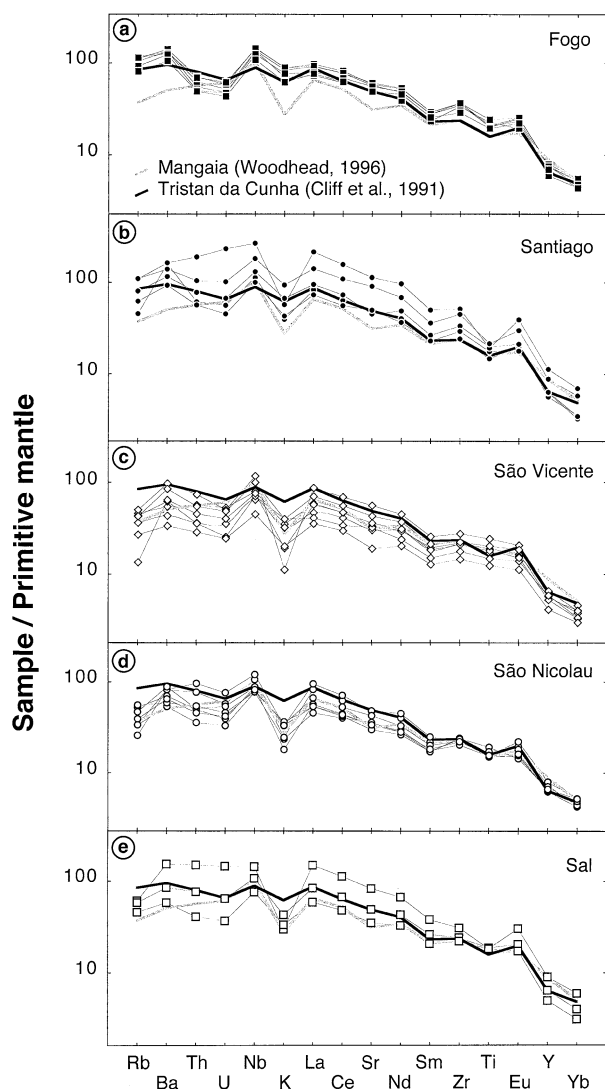


Fig. 5. Abundances of trace elements in samples from (a) Fogo, (b) Santiago, (c) São Vicente, (d) São Nicolau, and (e) Sal normalized to the primitive mantle values of Hofmann (1988).

S-07 from Sal) together with “melting” experiments. $^4\text{He}/^3\text{He}$ isotopic ratios (crushing) display reproducible values for olivines and pyroxenes.

The helium isotopic results for Cape Verde basalts clearly define two geographical groups (Fig. 7a). Fogo ($R/R_A = 7.90$ – 8.40) and Santiago ($R/R_A = 7.66$ – 8.31) in the Southern Islands have MORB-like compositions, whereas the Northern Island basalts have more primitive He isotopic compositions ($8.41 < R/R_A < 15.73$), with the exception of a single sample from Sal (S-06; Table 4) with $R/R_A = 6.98$. The most primitive values ($R/R_A = 10.47$ – 15.73) are found for São Nicolau basalts, which also plot out of the “Northern Island” trend for Pb isotopes (Fig. 6). The strong homogeneity in helium ratios measured in samples from Fogo island cannot be related to a sampling bias, as both pre- and post-caldera basalts covering a large surface area (Fig. 2) have been analyzed. Low helium ratios ($^4\text{He}/^3\text{He}$ He down to 52,000; $R/R_A = 13.8$) associated with relatively radiogenic lead ($^{206}\text{Pb}/^{204}\text{Pb} = 18.90$ – 19.63 ; $^{207}\text{Pb}/^{204}\text{Pb} =$

15.526 – 15.621 ; and $^{208}\text{Pb}/^{204}\text{Pb} = 38.694$ – 39.272) were measured by Christensen et al. (2001) for the Northern Islands in their study of Santo Antão island. They were not able, however, to define the MORB-like helium signature for the Southern Islands because they only measured two samples from Fogo.

6. FINGERPRINTING MANTLE SOURCES

Modeling presented in section 4 based on trace element data may suggest that basalts from the Northern and Southern Islands mainly represent the partial melting in variable degrees of two distinct oceanic lithospheric sources. However, as trace element patterns (Fig. 5) and Sr-Pb-He isotope ratios (section 5) are also very similar to those of HIMU-like and EMI-like mantle end-members, we will interpret all the variations observed in this study in terms of mixing between components. This assumption is in agreement with the existence of positive trends between Th/Nb ratios and Pb isotopic compositions for both the Northern and Southern Islands of the Cape Verde archipelago (Fig. 8), which demonstrates that Th/Nb vs. Th/Tb variations here do not result solely from melting processes.

As pointed out by Gerlach et al. (1988), the fact that the isotopic signatures of samples from the Southern and Northern Islands barely overlap suggests that mantle source heterogeneities exist at the scale of ~ 100 to 200 km beneath the Cape Verde archipelago. In principle, linear correlations in Pb-Pb space can be interpreted as simple binary mixing between isotopically distinct reservoirs. In the Cape Verde archipelago three distinct groups are present (e.g., Fig. 6a), corresponding respectively to the Southern Islands, the Northern Islands and the São Nicolau basalts, which would require six end-members.

Figure 9 summarizes the Pb and Sr isotopic results obtained herein and compares them to a set of reference parameters, data from the literature and potential end-members. End-member labeled [1], sitting on the NHRL (Figs. 9a and 9b), is admittedly common to the Fogo-Santiago (Southern Islands) and São Vicente-Santo Antão (Northern Islands) trends. This end-member is also consistent with the Sr-Pb isotopic relationships (Fig. 9c); it has $^{206}\text{Pb}/^{204}\text{Pb}$ and $^{87}\text{Sr}/^{86}\text{Sr}$ ratios of ~ 19.75 and ~ 0.70333 , respectively. The other end-members required to explain the data distribution (labeled [2] to [5] on Fig. 9) are: [2] $^{206}\text{Pb}/^{204}\text{Pb} < 18.80$ and $^{87}\text{Sr}/^{86}\text{Sr} > 0.7039$; [3] $^{206}\text{Pb}/^{204}\text{Pb} \sim 19.00$ and $^{87}\text{Sr}/^{86}\text{Sr} \sim 0.7028$; [4] $^{206}\text{Pb}/^{204}\text{Pb} \sim 19.35$ and $^{87}\text{Sr}/^{86}\text{Sr} \sim 0.7034$; [5] $^{206}\text{Pb}/^{204}\text{Pb} \sim 19.65$ and $^{87}\text{Sr}/^{86}\text{Sr} \sim 0.7028$.

We interpret the variations of the isotopic data in terms of five distinct components: recycled oceanic crust, lower mantle, subcontinental lithosphere, depleted mantle and oceanic crustal material. End-member [1] is thought to result from the mixture between 1.6-Ga recycled oceanic crust and lower mantle material, whereas end-member [2] is related to subcontinental lithospheric mantle: the mixing in variable proportions between these two end-members leads to the isotopic variations that are observed in the Southern Islands. End-member [3] corresponds to the locally depleted upper mantle; it explains, coupled with end-member [1], the variations found at São Vicente and Santo Antão (Northern Islands). We infer that end-member [4] is only slightly different from [1], as it also results from lower mantle

Table 3. Strontium and lead isotopic compositions of Cape Verde basalts.

Sample	$^{87}\text{Sr}/^{86}\text{Sr}$	$^{206}\text{Pb}/^{204}\text{Pb}$	$^{207}\text{Pb}/^{204}\text{Pb}$	$^{208}\text{Pb}/^{204}\text{Pb}$
<i>Fogo</i>				
F-01	0.703685 (18)	19.105 (8)	15.553 (9)	38.884 (31)
F-02 (A)	0.703723 (23)	19.062 (11)	15.563 (14)	38.858 (47)
F-02 (B)		19.067 (8)	15.571 (9)	38.903 (31)
F-06	0.703738 (20)	18.900 (8)	15.539 (9)	38.731 (31)
F-07	0.703789 (19)	18.882 (11)	15.530 (14)	38.701 (46)
F-08a	0.703734 (22)	18.954 (8)	15.563 (9)	38.836 (31)
F-08b (A)	0.703734 (22)	18.936 (8)	15.560 (9)	38.818 (31)
F-08b (B)		18.937 (8)	15.556 (9)	38.810 (31)
F-10	0.703616 (24)	19.133 (8)	15.560 (9)	38.917 (31)
F-11 (A)	0.703665 (21)	19.072 (8)	15.567 (9)	38.938 (31)
F-11 (B)		19.081 (8)	15.565 (9)	38.957 (31)
F-12 (A)	0.703625 (20)	19.144 (8)	15.577 (9)	38.974 (31)
F-12 (B)		19.139 (8)	15.579 (9)	38.973 (31)
F-12 (C)		19.145 (8)	15.577 (9)	38.978 (31)
F-13	0.703715 (19)	19.109 (8)	15.552 (9)	38.901 (31)
F-14	0.703758 (19)	18.935 (8)	15.549 (9)	38.772 (31)
F-15 (A)	0.703738 (22)	18.923 (11)	15.544 (14)	38.783 (47)
F-15 (B)		18.937 (8)	15.558 (9)	38.797 (31)
F-16	0.703764 (19)	18.932 (8)	15.537 (9)	38.752 (31)
F-18	0.703546 (20)	19.220 (8)	15.563 (9)	38.914 (31)
F-20	0.703722 (22)	19.062 (11)	15.548 (14)	38.822 (47)
F-21	0.703727 (18)	19.020 (8)	15.554 (9)	38.832 (31)
F-22	0.703656 (21)	19.094 (8)	15.561 (9)	38.898 (31)
F-24	0.703761 (18)	18.969 (11)	15.562 (14)	38.804 (47)
<i>Santiago</i>				
ST-02	0.703486 (22)	19.308 (12)	15.567 (14)	39.001 (47)
ST-06	0.703516 (19)	19.374 (12)	15.575 (14)	39.097 (47)
ST-08		19.398 (12)	15.580 (14)	39.190 (47)
ST-09	0.703510 (18)	19.216 (12)	15.549 (14)	39.014 (47)
ST-10		19.095 (11)	15.539 (14)	38.905 (47)
<i>São Vicente</i>				
SV-01	0.703212 (21)	19.639 (12)	15.594 (14)	39.361 (47)
SV-02	0.703284 (16)	19.273 (12)	15.619 (14)	38.995 (47)
SV-02 L	0.703222 (19)			
SV-03	0.703210 (20)	19.187 (12)	15.571 (14)	38.763 (47)
SV-03 L	0.703161 (20)			
SV-05	0.703256 (25)	19.692 (12)	15.610 (14)	39.270 (47)
SV-09	0.703050 (16)	19.676 (12)	15.618 (14)	39.337 (47)
SV-10	0.703120 (20)	19.357 (12)	15.578 (14)	38.964 (47)
SV-10 L	0.703115 (21)			
SV-12	0.703279 (19)	19.677 (12)	15.608 (14)	39.401 (47)
<i>São Nicolau</i>				
SN-02	0.702990 (18)	19.526 (12)	15.603 (14)	38.984 (47)
SN-03	0.703356 (20)	19.406 (12)	15.570 (14)	38.946 (47)
SN-05	0.703067 (18)	19.489 (12)	15.573 (14)	38.953 (47)
SN-10	0.703050 (16)	19.538 (12)	15.586 (14)	38.964 (47)
SN-11	0.703130 (18)	19.464 (12)	15.580 (14)	38.961 (47)
SN-13	0.703115 (15)	19.472 (12)	15.589 (14)	38.981 (47)
SN-18	0.703222 (23)	19.446 (12)	15.580 (14)	38.939 (47)
<i>Sal</i>				
S-03	0.703131 (19)	19.442 (12)	15.575 (14)	38.927 (47)
S-06		19.360 (12)	15.564 (14)	38.990 (47)
S-07		19.363 (12)	15.582 (14)	39.004 (47)

Numbers in parentheses are 2σ errors referring to the last significant digits. Leached samples are suffixed "L".

material and recycled oceanic crust, the latter being younger (~1.1 Ga). Lastly, end-member [5] is interpreted as being oceanic crustal material with isotopic characteristics of unaltered Jurassic MORB. These last two end-members create the variations found at São Nicolau. Links between end-members [1] to [5] and the different components listed above will be discussed in detail in the following sections.

6.1. HIMU Signatures of the Northern Islands

Gerlach et al. (1988), Davies et al. (1989) and Christensen et al. (2001) investigated the nature of end-member [1]. These authors all concluded the presence of a HIMU or a "young HIMU" component made of ancient recycled oceanic crust. This scenario was modeled for Pb isotopes using a two-stage

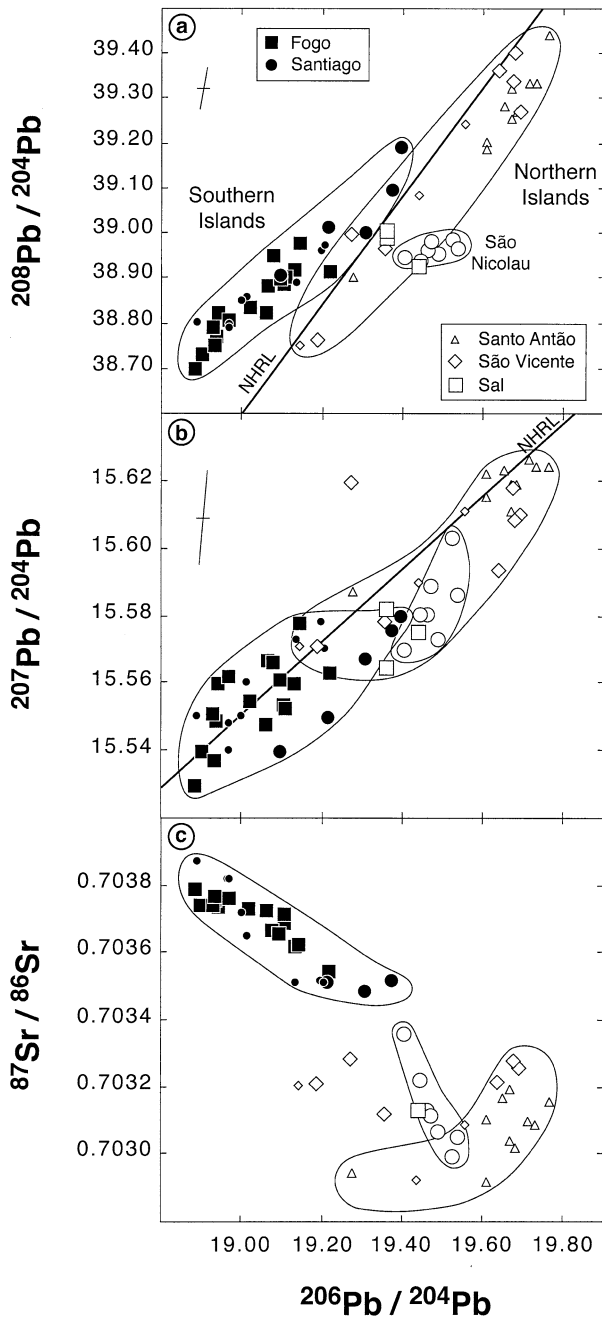


Fig. 6. (a) $^{208}\text{Pb}/^{204}\text{Pb}$, (b) $^{207}\text{Pb}/^{204}\text{Pb}$, and (c) $^{87}\text{Sr}/^{86}\text{Sr}$ vs. $^{206}\text{Pb}/^{204}\text{Pb}$ diagrams for Cape Verde samples. Large symbols identify results from this study; small symbols correspond to data in the literature (Gerlach et al., 1988). Open symbols = Northern Islands; filled symbols = Southern Islands. NHRL = Northern Hemisphere Reference Line (Hart, 1984). Typical 2σ analytical errors for Pb isotope ratios are shown in upper left hand corner.

model and the following parameters: recycled oceanic crust = 1 to 1.6 Ga; initial Canyon Diablo values; $\mu_1 \sim 8$, $\mu_2 = \text{mean } \mu$, $\kappa_1 \sim 3.8$, $\kappa_2 \sim 3.1$ and $T = 4.55$ Ga (Weaver, 1991; Chauvel et al., 1992; Thirlwall, 1997). The modeling does not yield appropriate Pb isotopic compositions for end-member [1]. As can be seen in Figure 9a, the recycled oceanic crust com-

ponent displays, in the best case (i.e., for a recycling age of ~ 1.1 Ga), a $^{208}\text{Pb}/^{204}\text{Pb}$ ratio close to 39.0 for a $^{206}\text{Pb}/^{204}\text{Pb}$ of ~ 20.0 . In other words, it has a $\Delta 8/4$ value ($\Delta 8/4$ is the deviation of the $^{208}\text{Pb}/^{204}\text{Pb}$ ratio relative to the NHRL for a given $^{206}\text{Pb}/^{204}\text{Pb}$, as defined by Hart, 1984) < -69 , instead of -7 as predicted by the position of end-member [1]. Thus recycling of oceanic crust alone cannot result in the end-member common to the Fogo-Santiago and the São Vicente-Santo Antão trends, and mixing with another component is required to explain its isotopic composition. Mixing of recycled oceanic crust with Atlantic depleted MORB mantle (DMM) material will not increase the $\Delta 8/4$ value up to -7 . This is because: (1) the DMM Pb isotopic composition has a $\Delta 8/4$ near zero; and (2) its involvement must be limited otherwise the $^{206}\text{Pb}/^{204}\text{Pb}$ ratio will not remain close to 20.0. In contrast, addition of materials such as sediments or lower mantle material would increase the $\Delta 8/4$ value as well as the $^{87}\text{Sr}/^{86}\text{Sr}$ ratio of end-member [1]. Recycled sediments (Weaver, 1991; Chauvel et al., 1992) display radiogenic $^{87}\text{Sr}/^{86}\text{Sr}$ (≥ 0.710), low $^{206}\text{Pb}/^{204}\text{Pb}$ (≤ 18) and high $\Delta 8/4$ (> 100), whereas lower mantle material is expected to display an isotopic composition close to that of the Bulk Silicate Earth i.e., $^{87}\text{Sr}/^{86}\text{Sr} = 0.70462$, $^{206}\text{Pb}/^{204}\text{Pb} = 18.34$ and $^{208}\text{Pb}/^{204}\text{Pb} = 39.05$ ($\Delta 8/4 = 125$) (Allègre and Lewin, 1989). Evidence for the involvement of the lower mantle rather than recycled sediments in the source of the Cape Verde basalts is presented in section 6.2.

In an alternative scenario, Kokfelt et al. (1998) proposed that the HIMU end-member could correspond to subcontinental mantle that was metasomatized by carbonatitic fluids before the opening of the Atlantic Ocean. This model is supported by the presence of: (1) carbonatite intrusions on some Cape Verde islands (carbonatites are rare in oceanic settings and have only been found on the Canary and Cape Verde islands e.g., Allègre et al., 1971; Hoernle et al., 2002); and (2) the HIMU end-member in Cape Verde basalts has high U/Pb, U/Th and Zr/Hf ratios, which are typical features of carbonatites. However, Cape Verde carbonatites (Gerlach et al., 1988; Hoernle et al., 2002) do not yield Pb isotopic compositions corresponding to end-member [1] (Figs. 9a and 9b). Furthermore, Cape Verde basalts yield Zr/Hf ratios in the range of 36 to 59 (mean = 45; data from Gerlach et al., 1988, and Table 1). These are values similar to those reported by Turner et al. (1997) for the Azores archipelago (41–50; mean = 44) where no carbonatites occur. Higher Zr/Hf ratios, $\gg 50$ (Woodhead, 1996), would be expected if carbonatized mantle was present in the source of the Cape Verde basalts. In the same way, the lack of correlation between Zr/Hf and $^{206}\text{Pb}/^{204}\text{Pb}$ (figure not shown) excludes the involvement of a carbonatite-like component in the most radiogenic $^{206}\text{Pb}/^{204}\text{Pb}$ samples of the Cape Verde archipelago. Such a conclusion was also defended by Jørgensen and Holm (2002) in a recent study of São Vicente island. They showed that two distinct sources were required to explain the HIMU-like signature of basalt and carbonatite samples, even if carbonatitic fluids could affect some basalt compositions to a lesser extent.

The recycling of ~ 1.6 -Ga-old oceanic crust with carbonate sediments was recently proposed by Hoernle et al. (2002) to explain major, trace element and isotopic variations in calcio-carbonatites (that is excluding dolomitic-carbonatites which may be secondary in origin) from the Cape Verde archipelago.

Table 4. Helium concentrations (in 10^{-8} cm³ STP/g) and blank corrected isotopic ratios.

Sample		Weight (g)	⁴ He ($\times 10^{-8}$)	R/R_A	σ	⁴ He/ ³ He	σ	% blank
<i>Fogo</i>								
F-01	Ol.	0.297	0.70	8.53	0.09	84,706	894	2.4
	CPX	0.286	0.24	6.88	0.13	105,021	1984	7.3
F-02	Ol.	0.346	0.33	7.90	0.12	91,519	1437	4.4
	CPX	0.328	0.75	7.91	0.09	91,322	1062	2.0
	mp	0.306	0.41	4.89	0.07	147,669	1992	4.0
F-05	Ol.	0.186	0.69	7.53	0.09	95,955	1147	3.9
	CPX	0.057	1.01	8.56	0.19	84,409	1874	8.7
F-07	Ol.	0.100	5.12	8.28	0.06	87,264	632	1.0
	mp	0.083	1.93	7.90	0.09	91,450	1019	3.1
F-08	Ol.	0.088	2.67	8.06	0.10	89,646	1112	2.1
	mp	0.066	0.16	4.66	0.50	155,185	16,498	46.1
F-11	Ol.	0.294	0.10	6.31	0.23	114,562	4087	16.6
	mp	0.262	0.13	8.44	0.32	85,609	3286	14.2
	Ol.	0.281	0.12	7.23	0.26	99,909	3550	14.7
	<i>Re-crush</i>		0.04	9.54	0.85	75,746	6773	46.8
	Ol.	0.156	0.38	8.04	0.21	89,869	2347	8.5
F-13	Ol.	0.126	0.30	7.76	0.29	93,147	3458	13.3
	<i>Re-crush</i>		0.05	6.90	0.98	104,777	14,860	83.7
	CPX	0.211	0.89	7.74	0.11	93,352	1327	2.6
	mp	0.186	0.44	5.90	0.13	122,486	2762	6.2
	CPX	0.252	1.45	7.96	0.09	90,772	1026	1.4
F-15	Ol.	0.083	4.39	8.15	0.07	88,677	762	1.4
F-16	Ol.	0.076	4.58	8.24	0.08	87,687	851	1.4
F-18	Ol.	0.244	1.49	7.91	0.06	91,346	693	1.4
F-20	Ol.	0.171	0.36	8.40	0.14	86,068	1425	8.1
F-21	Ol.	0.075	1.37	8.04	0.12	89,869	1341	4.9
F-24	Ol.	0.163	1.23	7.76	0.10	93,135	1152	2.5
<i>Santiago</i>								
ST-02	Ol.	0.079	0.17	8.24	0.42	87,719	4515	38.5
ST-06	Ol.	0.157	0.04	3.90	0.80	185,505	38,054	75.0
	<i>Re-crush</i>		0.02	7.66	2.77	94,327	34,160	159.2
	mp	0.135	0.48	29.20	0.27	24,741	231	7.7
ST-08	Ol.	0.193	0.19	8.31	0.23	86,917	2405	13.4
	mp	0.168	0.58	6.36	0.21	113,697	3686	5.2
ST-09	CPX	0.095	0.11	1.38	0.51	522,824	192,938	47.6
	mp	0.075	15.28	0.18	0.01	4,128,819	117,966	0.4
<i>São Vicente</i>								
SV-01	Ol.	0.230	1.01	9.07	0.11	79,628	965	2.1
	<i>Re-crush</i>		0.06	6.45	0.34	111,970	5865	34.3
SV-02	Ol.	0.194	0.60	9.95	0.12	72,617	876	4.3
	CPX	0.211	0.25	9.07	0.18	79,663	1581	9.5
	<i>Re-crush</i>		0.09	9.82	0.43	73,579	3222	25.8
SV-03	Ol.	0.159	0.92	10.83	0.64	66,717	3943	3.4
SV-05	Ol.	0.177	0.06	10.70	0.83	67,527	5238	48.4
	<i>Re-crush</i>		0.02	10.81	1.52	66,840	9398	136.5
SV-09	Ol.	0.161	0.64	11.08	0.18	65,211	1059	4.8
SV-10	Ol.	0.092	0.43	12.27	0.77	58,887	3695	12.8
SV-12	Ol.	0.097	1.41	8.41	0.13	85,905	1369	3.7
<i>São Nicolau</i>								
SN-02	Ol.	0.302	5.00	12.94	0.04	55,838	173	0.3
	mp	0.245	4.06	12.87	0.07	56,133	301	0.5
SN-03	Ol.	0.173	0.41	14.03	0.20	51,515	742	7.1
	<i>Re-crush</i>		0.02	10.87	1.87	66,447	11,421	132.2
SN-05	Ol.	0.148	1.88	15.24	0.06	47,411	187	1.8
SN-10	Ol.	0.257	2.33	15.73	0.09	45,928	251	0.8
	<i>Re-crush</i>		0.29	15.58	0.19	46,367	571	6.7
SN-11	Ol.	0.044	1.39	10.47	0.21	69,031	1359	8.1
SN-13	Ol.	0.330	0.27	12.00	0.14	60,212	702	5.7
<i>Sal</i>								
S-03	Ol.	0.058	0.40	9.55	0.30	75,659	2377	21.5
S-06	Ol.	0.280	1.03	6.98	0.05	103,590	772	1.7
S-07	Ol.	0.237	0.94	9.97	0.12	72,486	880	2.2
	<i>Re-crush</i>		0.34	9.74	0.13	74,175	952	6.2
	mp	0.200	2.52	42.64	0.16	16,947	64	1.0
	Ol.	0.166	1.56	9.98	0.13	72,416	973	1.9

R/R_A is the ³He/⁴He ratio normalized to the atmospheric value of 1.384×10^{-6} . Uncertainty in the helium concentrations is $\sim 5\%$. The last column gives the percentages of ⁴He blank contribution, $\sim 5 \times 10^{-11}$ cm³ STP, relative to sample content. Measurements were completed on olivine (Ol.) and clinopyroxene (CPX). "Re-crush" identifies samples which were crushed a second time, sequentially, in order to verify for complete extraction and identify any contributions from radiogenic helium. The experiments done by melting of remaining crushed powders are labeled "mp".

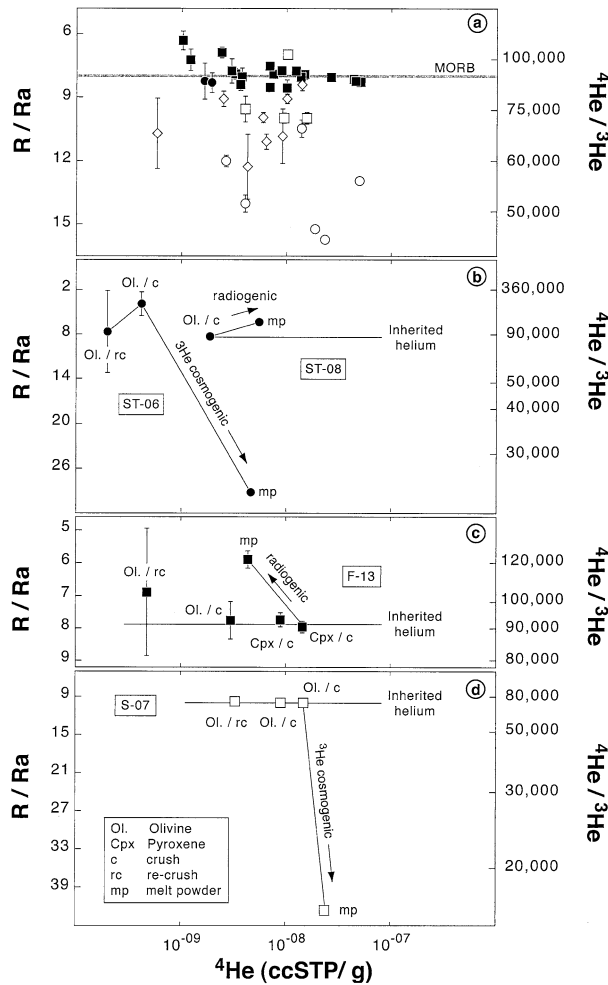


Fig. 7. Diagrams of R/R_A (and absolute $^4\text{He}/^3\text{He}$) ratios vs. ^4He concentrations for studied Cape Verde basalts. (a) Results for all olivine and pyroxene separates from samples analyzed using the crushing protocol compared to the MORB reference composition; symbols as in Figure 6. (b-d) Results for olivines and pyroxenes from samples ST-06, ST-08, F-13 and S-07; key to symbols and analytical steps in (d). The crushing of olivines and pyroxenes from samples F-13 and S-07 yields similar R/R_A ratios. This implies that the $^4\text{He}/^3\text{He}$ ratios obtained by crushing are representative of the magmatic values (inherited helium). Melt products (mp) indicate that excesses of radiogenic ^4He and cosmogenic ^3He are present in the samples.

In the following sections we, too, will use the figure of 1.6 Ga for the recycled oceanic crust component(s).

6.2. Lower Mantle Material in the Plume Source

The low $^4\text{He}/^3\text{He}$ ratios determined in basalts from the Northern Islands (R/R_A up to 15.73) imply the involvement of a lower mantle component in the plume source. Mid-ocean ridge basalts have similar $^4\text{He}/^3\text{He}$ values of $88,000 \pm 5000$ ($R/R_A \sim 8 \pm 1$; cf. Kurz et al., 1982; Allègre et al., 1995) representative of the outgassed upper mantle; conversely, OIB values as low as 17,000 ($R/R_A \sim 43$; cf. Breddam and Kurz, 2001) are attributed to a relatively undegassed reservoir thought to be the lower mantle (Kurz et al., 1982).

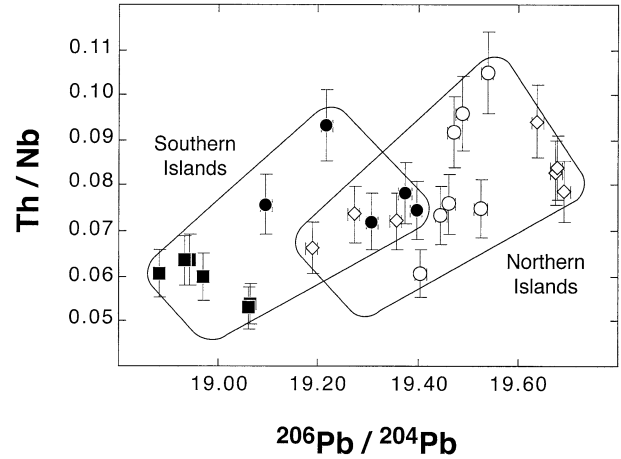


Fig. 8. Th/Nb vs. $^{206}\text{Pb}/^{204}\text{Pb}$ variations for Cape Verde samples. The two positive trends which are observed for basalts from the Northern and Southern Islands suggest that Th/Nb ratios do not reflect melting processes, but rather mixing between two distinct end-members.

We assume that present-day Pb and Sr isotope compositions of the lower mantle (LM) are similar to those of the Bulk Silicate Earth (BSE), reflecting binary mixing between BSE material and a fraction of depleted mantle. Mass balance calculations which are detailed in the Appendix lead to the following isotopic signature: $^{206}\text{Pb}/^{204}\text{Pb} = 18.30$, $^{207}\text{Pb}/^{204}\text{Pb} = 15.546$ ($\Delta 7/4 \sim 7$), $^{208}\text{Pb}/^{204}\text{Pb} = 38.97$ ($\Delta 8/4 \sim 120$) and $^{87}\text{Sr}/^{86}\text{Sr} = 0.70429$. This allows us to verify that the Pb and Sr isotopic compositions of end-member [1] can be explained by mixing between 1.6-Ga recycled oceanic crust and lower mantle material. Assuming that the 1.6-Ga recycled oceanic crust component (ROC) had $^{206}\text{Pb}/^{204}\text{Pb} = 21.17$, $^{207}\text{Pb}/^{204}\text{Pb} = 15.72$, $^{208}\text{Pb}/^{204}\text{Pb} = 39.92$ ($\mu_1 = 8$, $\mu_2 = 21$, $\kappa_1 = 3.8$ and $\kappa_2 = 3.05$) and $^{87}\text{Sr}/^{86}\text{Sr} = 0.70290$, solid-state mixing of ROC and LM in the proportion of 42:58 (with Pb contents of 0.2 and 0.3 ppm, and Sr contents of 20 and 60 ppm, respectively) yields Pb and Sr isotopic ratios close to those expected for end-member [1]: $^{206}\text{Pb}/^{204}\text{Pb} = 19.758$; $^{207}\text{Pb}/^{204}\text{Pb} = 15.636$ ($\Delta 7/4 = 0.3$); $^{208}\text{Pb}/^{204}\text{Pb} = 39.454$ ($\Delta 8/4 = -6.1$); and $^{87}\text{Sr}/^{86}\text{Sr} = 0.70334$.

In the same way, assuming a ^4He content of $1 \times 10^{-4} \text{ cm}^3 \text{ STP/g}$ (Allègre et al., 1986) and a $R/R_A \sim 43$ ($^4\text{He}/^3\text{He} = 16,800$) for lower mantle material as well as a ^4He production of $3 \times 10^{-5} \text{ cm}^3 \text{ STP/g}$ (cf. radioactive production equation in Moreira et al., 1999, with $[U] = 0.09 \text{ ppm}$ and $\text{Th}/U = 3.03$) and $R/R_A = 0$ for the recycled oceanic crust component, the mixture in the proportion of 42:58 yields a $^4\text{He}/^3\text{He}$ ratio of $\sim 20,600$ ($R/R_A \sim 35$) for end-member [1] (Fig. 10).

Lower mantle material is possibly entrained into plumes by viscous coupling from a boundary layer in a mass proportion which does not exceed 10% (Davaille, 1999). Recent numerical simulations by Farnetani et al. (2002) have shown that heterogeneities present in the source region of plumes evolve as narrow filaments while rising, but are not homogenized. End-member [1], however, presents a well-constrained signature for both Pb and Sr isotopes suggesting that proportions of recycled oceanic crust and lower mantle material are relatively constant over the time interval of the

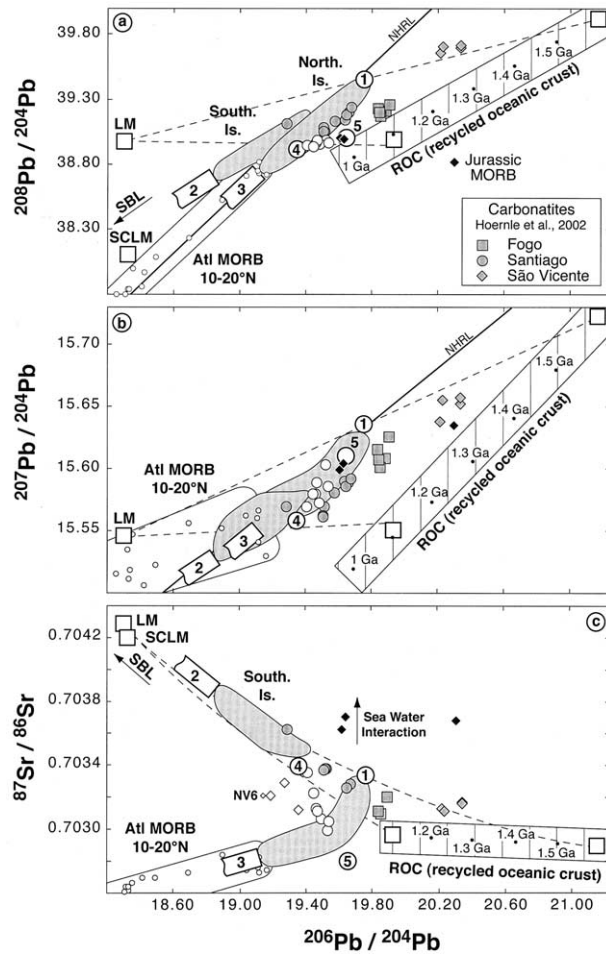


Fig. 9. Pb and Sr isotopic compositions of studied Cape Verde basalts in relation to potential end-members (labeled [1] to [5]) and data from the literature. (a) $^{208}\text{Pb}/^{204}\text{Pb}$ vs. $^{206}\text{Pb}/^{204}\text{Pb}$; (b) $^{207}\text{Pb}/^{204}\text{Pb}$ vs. $^{206}\text{Pb}/^{204}\text{Pb}$; and (c) $^{87}\text{Sr}/^{86}\text{Sr}$ vs. $^{206}\text{Pb}/^{204}\text{Pb}$ diagrams. Grey fields = data from the Southern and Northern Island groups (cf. Fig. 6). Large open circles = data for São Nicolau basalts. Small open circles = Atlantic MORB collected between latitudes 10 and 20°N (Dosso et al., 1993). Black diamonds = Jurassic MORB sampled on Santiago island (Gerlach et al., 1988). Grey symbols = carbonatites on the Fogo, Santiago and São Vicente islands (Hoernle et al., 2002). NHRL = Northern Hemisphere Reference Line of Hart (1984); LM = Lower Mantle (see Appendix for calculations); SCLM = SubContinental Lithospheric Mantle from Zartman and Haines (1988); and SBL = Smoky Butte Lamproites (Fraser et al., 1985/1986). Striped fields = Recycled Oceanic Crust (ROC), considering a two-stage model with $\mu_1 = 8$, $\mu_2 = 21$, $\kappa_1 = 3.8$, $\kappa_2 = 3.05$ and an age ranging from 1 to 1.6 Ga. End-member [1] is interpreted as resulting from the mixture between 1.6 Ga recycled oceanic crust and lower mantle material; end-members [2] and [3] correspond to subcontinental lithosphere and depleted local upper mantle, respectively; end-member [4] is also interpreted as resulting from the mixture between oceanic crust and lower mantle, but recycling age is younger (~ 1.1 Ga); end-member [5] is thought to be oceanic crustal material having isotopic characteristics of unaltered Jurassic MORB.

samples analyzed by Gerlach et al. (1988) and this study. These constant proportions imply a two-stage history for Cape Verde basalts: firstly end-member [1] has to be generated, possibly in a magma chamber. Secondly, it is mixed

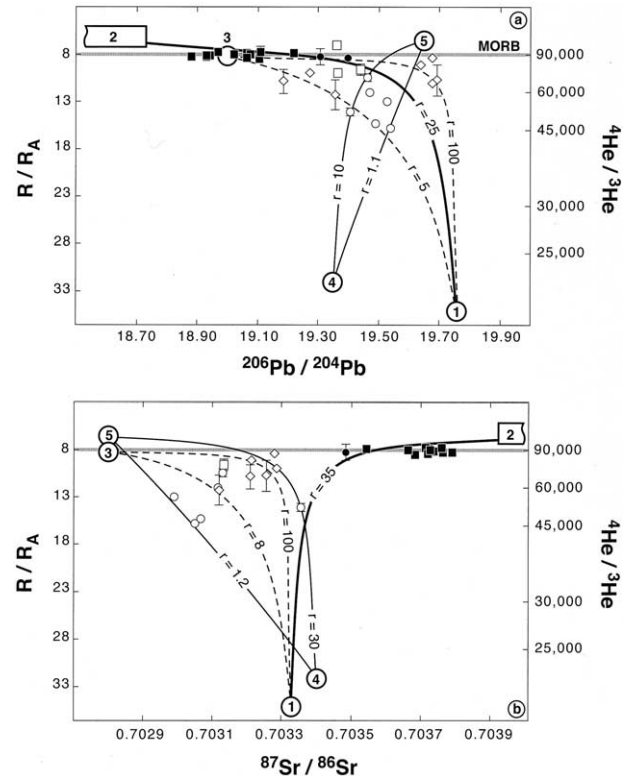


Fig. 10. (a) R/R_A ($^4\text{He}/^3\text{He}$) vs. $^{206}\text{Pb}/^{204}\text{Pb}$; and (b) R/R_A ($^4\text{He}/^3\text{He}$) vs. $^{87}\text{Sr}/^{86}\text{Sr}$ for Cape Verde samples (symbols as in Fig. 6). Potential end-members which allow observed isotopic variations to be explained for both the Northern and Southern Islands are labeled [1] to [5] (see Fig. 9). Also reported are the r -values (Langmuir et al., 1978) which determine the curvature of mixing lines: these are the $(\text{He}/\text{Pb})_a/(\text{He}/\text{Pb})_b$ and $(\text{He}/\text{Sr})_a/(\text{He}/\text{Sr})_b$ ratios between two end-members a and b.

in variable proportions with another component, whose identity depends on the group of islands which is considered. Consequently, the proportions of recycled oceanic crust and lower mantle material which are required to model the isotopic composition of end-member [1] (42:58) do not necessarily correspond to the proportions that are present in the Cape Verde plume.

It should be noted that recycling of oceanic crust is possibly accompanied by recycling of oceanic lithosphere (Moreira and Kurz, 2001). The latter has a low Pb content as well as an unradiogenic signature. Consideration of recycled oceanic crust (ROC) and lithosphere together instead of oceanic crust alone results in a less radiogenic Pb composition for the ROC component (Fig. 9); it also decreases the proportion of lower mantle material which is required to model the isotopic composition of end-member [1]. Nevertheless its $^4\text{He}/^3\text{He}$ ratio will remain low (close to 20,000) due to the high ^3He content of lower mantle material.

To summarize, we propose that end-member [1] corresponds to 1.6-Ga recycled oceanic crust, to which is added a fraction of lower mantle material. This model is in agreement with Christensen et al. (2001), who also proposed the involvement of recycled oceanic crust and lower mantle.

6.3. Subcontinental Lithospheric Material as the EMI End-Member

The trace element patterns for Fogo and Santiago are very similar to those of Tristan da Cunha lavas (Fig. 5), suggesting that end-member [2] is an EMI-like source. Gerlach et al. (1988) and Davies et al. (1989) explained this feature by the occurrence of subcontinental mantle beneath the Southern Islands. However, they did not address the question of whether such material was present beneath the Cape Verde archipelago as a passive heterogeneity or was supplied by the plume. In their study of Fogo, Kokfelt et al. (1998) also argued for a subcontinental origin of the EMI-like signature, proposing that it represented delaminated continental lithosphere left behind in the mantle during the early opening of the Atlantic, following the model of Cohen and O'Nions (1982) and McKenzie and O'Nions (1983). Finally, Christensen et al. (2001) also concluded that an EMI component must be present in the source of Southern Island basalts. Linking subcontinental lithosphere to end-member [2] is supported by the high Ba/La (7–23, mean = 14) and low La/Nb ratios (0.54–0.89, mean = 0.71) measured in Fogo and Santiago basalts (data from Gerlach et al., 1988, and this study). Furthermore, coupled with the fact that $^{143}\text{Nd}/^{144}\text{Nd}$ ratios measured in Fogo basalts are low (~ 0.51260 , cf. Gerlach et al., 1988; Kokfelt et al., 1998), both Fogo and Santiago samples are aligned in Pb-Pb space (Figs. 9a and 9b) with the expected composition of the subcontinental lithosphere (Zartman and Haines, 1988) as well as with Smoky Butte lamproites (data from Fraser et al., 1985/1986) which are thought to sample this reservoir (Hawkesworth et al., 1990). Smoky Butte lamproites have been interpreted as sampling subcontinental lithosphere enriched by the introduction of small volumes of silicate melts. They can be modeled for Pb isotopes using a two-stage evolution where decreasing of the μ_2 value relative to μ_1 reflects the low U/Pb ratio in the enriching agent or the stabilization of low U/Pb phases (Fraser et al., 1985/1986). Their Pb isotopic compositions, however, plot quite far from the expected values of end-member [2], and do not agree with trace element data which suggest a high proportion of the EMI-like end-member relative to [1] in the source of the Southern Islands. Using a similar evolution ($\mu_2 < 7.5$, cf. Fraser et al., 1985/1986) for a second stage between 1 and 2.5 Ga does not allow the generation of radiogenic Pb isotopic ratios ($^{206}\text{Pb}/^{204}\text{Pb}$ close to 18.5) which would remain aligned with those of Fogo and Santiago. Thus a more complex evolution where a decrease of the U/Pb ratio is followed by a more recent increase (Fraser et al., 1986/1986) has to be considered. In addition to unradiogenic Pb, Smoky Butte lamproites also display relatively high Sr values ($0.70587 < ^{87}\text{Sr}/^{86}\text{Sr} < 0.70633$) which are consistent with Fogo and Santiago data (Fig. 9c). For helium isotopes, we refer to the recent study of Gautheron and Moreira (2002) who demonstrate the homogeneous signature of the subcontinental mantle with a mean $^4\text{He}/^3\text{He}$ ratio of $118,000 \pm 15,500$ ($R/R_A = 6.1 \pm 0.9$). Our measurements show lower values ($^4\text{He}/^3\text{He} \sim 90,000$) which certainly reflect mixing with the lower mantle material which makes up end-member [1]. It is surprising, however, to obtain the $^4\text{He}/^3\text{He}$ ratio of MORB, although this can be viewed in relation to Hawaiian postshield lavas which display MORB-

like helium values (Kurz et al., 1996) but Sr and Pb isotopic signatures, demonstrating the involvement of sediments.

6.4. Mixing With Depleted Mantle Material

Albeit the least radiogenic samples from São Vicente and Santo Antão plot far from the depleted mantle value (DMM), the Northern Islands (excluding São Nicolau) point toward the composition of the nearest Atlantic MORB (10–20°N) in Pb-Pb space (Figs. 9a and 9b). The latter were interpreted as a mixture between a regional enriched component and DMM, but are not related to the Cape Verde plume (Dosso et al., 1993). Thus end-member [3] could represent locally depleted mantle material, as previously proposed by Gerlach et al. (1988) who argued that a minor DMM contribution would even explain the low Ba/La (6–16, mean = 11) and Ba/Nb (5–10, mean = 8) ratios measured in São Vicente and Santo Antão basalts.

It is, however, noteworthy that samples SV-02, SV-03, SV-10 and alkali basalt NV6 (Gerlach et al., 1988) from São Vicente display $^{87}\text{Sr}/^{86}\text{Sr}$ ratios higher than that expected from a DMM contribution (Fig. 9c). These four samples are all Quaternary or post-erosional basalts. Several authors have proposed that Hawaiian post-erosional lavas may not represent the plume itself, but rather the oceanic lithosphere (e.g., Chen and Frey, 1985; Lassiter et al., 2000). Low $^4\text{He}/^3\text{He}$ ratios measured for the three São Vicente basalts ($R/R_A = 9.95\text{--}12.27$) do not allow us to rule out significant melt input from the plume. Leaching experiments that were performed on these basalts, which were all collected near the ocean shore (Fig. 2), argue against seawater alteration, as leaching residues have Sr signatures comparable with those of the bulk samples (Table 3). It is more likely that high Sr values, coupled with less radiogenic Pb, relative to other São Vicente samples result from interaction with Quaternary sedimentary deposits belonging, together with recent lavas, to the “Monte Verde” complex as defined by Serralheiro (1976) and Trindade et al. (2001), which is where samples SV-03 and SV-10 were collected. Alternatively, these basalts could reflect carbonatite assimilation, as has been recently proposed for some lavas from São Vicente by Jørgensen and Holm (2002).

6.5. São Nicolau: Evidence for Oceanic Crustal Material Assimilation?

The Pb and Sr isotopic compositions of basalts from São Nicolau show small but significant variations defining good correlations in both Pb-Pb and Sr-Pb spaces (Fig. 6). The alignment of the data suggests binary mixing of isotopically distinct end-members. The end-members must differ in isotopic compositions from those postulated for São Vicente and Santo Antão lavas. Trace element characteristics (HIMU-like) are, however, quite similar for all the Northern Islands (Fig. 5).

As end-member [4] plots on the São Vicente-Santo Antão trend on the $^{208}\text{Pb}/^{204}\text{Pb}$ vs. $^{206}\text{Pb}/^{204}\text{Pb}$ diagram (Fig. 9a), its isotopic composition may result from the mixture of 1.6-Ga recycled oceanic crust and lower mantle material, to which is added some local upper mantle (see sections 6.2 and 6.4). Addition of depleted material should result in a decrease of the Sr isotope signature. However, a more radiogenic value is observed relative to [1], thus dismissing such a hypothesis for

the origin for end-member [4]. With respect to the observations related to trace elements (Fig. 5), it is more likely that end-member [4] results from the mixture of ancient recycled oceanic crust and lower mantle material only. Its Pb and Sr isotopic composition can be modeled, for example, with a younger recycled oceanic crust of 1.1 Ga. Indeed, using similar characteristics for both recycled oceanic crust and lower mantle to that described in section 6.2, solid-state mixing in the proportion of 52:48 yields isotopic ratios close to those expected for end-member [4] i.e., $^{206}\text{Pb}/^{204}\text{Pb} \sim 19.30$, $^{207}\text{Pb}/^{204}\text{Pb} \sim 15.55$, $^{208}\text{Pb}/^{204}\text{Pb} \sim 39.00$ and $^{87}\text{Sr}/^{86}\text{Sr} \sim 0.7033$ (Fig. 9). This also results in a $^4\text{He}/^3\text{He}$ composition of 22,600 ($R/R_A \sim 32$), consistent with the low helium ratios measured in São Nicolau samples (Fig. 10).

In their study of the Cape Verde archipelago, Gerlach et al. (1988) analyzed Late Jurassic basalts from Santiago which were interpreted as N-type “normal” MORB (Gerlach et al., 1988; Mendes and Silva, 2001). Their initial $^{143}\text{Nd}/^{144}\text{Nd}$ ratios range from 0.51282 to 0.51288 and are close to those expected for Late Jurassic MORB. However, their initial Sr isotopic compositions (0.70284–0.70340) are more radiogenic than expected, and were interpreted to reflect seawater alteration. Pb isotopic compositions, although heterogeneous, are radiogenic with $^{206}\text{Pb}/^{204}\text{Pb} = 19.611$ to 20.303, $^{207}\text{Pb}/^{204}\text{Pb} = 15.599$ to 15.635 and $^{208}\text{Pb}/^{204}\text{Pb} = 38.820$ to 39.004; $\Delta 7/4$ and $\Delta 8/4$ values are close to -1.5 and -35 (or lower), respectively, thus similar to those expected for end-member [5]. The $^{87}\text{Sr}/^{86}\text{Sr}$ ratio of unaltered Jurassic MORB can be estimated from both the measured $^{143}\text{Nd}/^{144}\text{Nd}$ and the Sr-Nd correlation defined by Cape Verde basalts (Gerlach et al., 1988). This yields a value of ~ 0.7028 which, coupled with Pb isotopic compositions, corresponds to end-member [5] in the $^{87}\text{Sr}/^{86}\text{Sr}$ vs. $^{206}\text{Pb}/^{204}\text{Pb}$ diagram (Fig. 9c). Based on isotopic arguments, we thus propose that São Nicolau samples could reflect the mixing between end-member [4] and oceanic crustal material having an isotopic signature similar to that of unaltered Jurassic MORB, and forming the deeper part of the basement beneath the Cape Verde Islands. Inferring that end-member [5] indeed represents Late Jurassic MORB, its helium isotopic composition must be MORB-like, or radiogenic, due to degassing at the ridge and possible production of radioactive ^4He (Fig. 10).

7. GEOCHEMICAL AND DYNAMIC ASPECTS OF THE CAPE VERDE PLUME

Kokfelt et al. (1998) proposed that the Cape Verde plume provided heat but not a distinct magma source. Evidence for lower mantle material in the Northern Island basalts with low $^4\text{He}/^3\text{He}$ signatures argues against such a model. Instead, we consider, based on Sr, Pb and He isotopes, the involvement of at least two components at the source of the plume: recycled oceanic crust and lower mantle material.

The Southern Island basalts reflect preferential mixing of this material (recycled oceanic crust + lower mantle) with relatively high proportions of subcontinental lithosphere, yielding EMI-like trace element patterns, displacing isotopic compositions toward less radiogenic Pb and higher Sr, and compensating for the primitive He signature of the lower mantle. Conversely, the Northern Island samples present isotopic compositions and trace element patterns which are consistent

with mixing between the two plume components and depleted material (Figs. 9 and 10).

Two distinct models can be proposed for the presence of the subcontinental lithospheric mantle (SCLM) component. In the first, the SCLM is present in the plume source: Gerlach et al. (1988) envisaged the storage of cold, dense subcontinental lithosphere at the 670-km discontinuity, the presence of whose signature is suppressed in the Northern Islands due to a lower degree of partial melting. In the second model, the SCLM is present in the oceanic lithosphere as a passive heterogeneity, and only the Southern Island basalts sample it. In such a case, the subcontinental lithosphere would have been recycled into the upper mantle by delamination during the opening of the Central Atlantic. One argument against model (1) is the necessity to preserve heterogeneities in the plume head: the SCLM on the one hand, recycled oceanic crust and lower mantle material on the other. However, a recent study has shown that heterogeneities initially present in the plume source are not homogenized during the ascent (Farnetani et al., 2002). Model (2) is also paradoxical; all samples from the Southern Islands (Fogo, Santiago as well as Maio, cf. Gerlach et al., 1988; Davies et al., 1989) present EMI-like characteristics, indicating that delaminated subcontinental lithosphere, although not sampled by the Northern Islands, occurs over a scale of at least ~ 150 km. This feature could be due to a tectonic control since the Northern and Southern Islands are related to different geological structures (see section 2).

The case of São Nicolau appears to be more problematic. Although basalts sampled on this island present trace element characteristics similar to those of São Vicente and Santo Antão, isotopic compositions for both Pb and Sr are significantly different. We propose that these compositions reflect mixing in constant proportions of ancient recycled oceanic crust (~ 1.1 Ga) and lower mantle, with assimilation of oceanic crustal material (Figs. 9 and 10). The involvement of recycled oceanic crust dating back to ~ 1.1 Ga, together with that of 1.6 Ga, has to be put in perspective with the source heterogeneity of the Cape Verde plume. Nevertheless, future analyses of new samples will help to ascertain the nature of the source components involved in São Nicolau volcanism.

Christensen et al. (2001) envisaged a source composition for Santo Antão similar to that proposed above (1.6-Ga recycled oceanic crust + lower mantle), although they suggested the presence of younger recycled oceanic crust (age not given), arguing that mixing of extreme HIMU (following the terminology of Thirlwall, 1997) and DMM material will not produce Pb isotopic compositions and $^{87}\text{Sr}/^{86}\text{Sr}$ ratios consistent with the most radiogenic samples of Santo Antão. They did not consider, however, that a lower mantle contribution would also increase $\Delta 7/4$ and $\Delta 8/4$ values and $^{87}\text{Sr}/^{86}\text{Sr}$ ratios without strongly decreasing the $^{206}\text{Pb}/^{204}\text{Pb}$. We thus think there is no clear evidence for the presence of a so-called “young HIMU” component in the source of Santo Antão basalts. Furthermore, the involvement of 1.6-Ga recycled oceanic crust in the source of the Cape Verde basalts is consistent with the model proposed by Hoernle et al. (2002) to explain the Sr and Pb isotopic compositions of Fogo, Santiago and São Vicente carbonates. Christensen et al. (2001) also proposed two hypotheses to explain the primitive He signatures of Santo Antão samples, either by entrainment of lower mantle material or He migra-

tion. Our model favors the first proposition, as it requires the involvement of lower mantle material for Pb and Sr isotopes.

8. SUMMARY

Pb-Sr-He isotope data show intra-island variations that require at least five distinct end-members for the source of the Cape Verde basalts. We propose that the isotopic compositions measured in the Northern Island samples are best explained by the mixture of 1.6-Ga recycled oceanic crust and lower mantle material which is added in variable proportions to entrained upper mantle material during the plume ascent. We also show that compositions of the Southern Islands require the presence of recycled oceanic crust and lower mantle material, albeit isotopic signatures are dominated by another component, identified as the subcontinental lithospheric mantle. Results for São Nicolau basalts are only slightly different from those of other Northern Islands (Santo Antão and São Vicente); they suggest, however, the assimilation of oceanic crustal material with an isotopic signature similar to that of unaltered Jurassic MORB. The model developed here confirms the previous studies of Gerlach et al. (1988) and Davies et al. (1989) who argued for the presence of old, recycled oceanic crust and subcontinental lithospheric material in the source of the Cape Verde basalts. It also extends their conclusions since we provide arguments for the involvement of the lower mantle and propose that both the HIMU- and EMI-like end-members may be present in the plume. Our model disagrees, however, with the conclusions of Kokfelt et al. (1998) and Christensen et al. (2001). The former restrict the plume to a heat source; the latter propose a younger age for the recycled oceanic crust (young HIMU) as well as an absence of (or minor) contribution from entrained depleted material for Santo Antão island.

Acknowledgments—The authors thank C. J. Allègre, B. Bourdon, A. Davaille, C. Farnetani, C. H. Langmuir and P. Schiano for constructive discussions and suggestions on the manuscript. R.D. is grateful to A. Simonetti for skilled assistance during the MC-ICP-MS measurements. Helium analyses were performed with the help of J. Curtice. R.D. was supported by a Lavoisier postdoctoral fellowship and M.M. by a WHOI fellowship. F. van Wik de Vries helped us for the quality of the manuscript. This paper was improved by critical comments by D. W. Peate and two anonymous reviewers. This is IPGP contribution 1889.

Associate editor: M. A. Menzies

REFERENCES

- Allègre C. J. (1987) Isotope geodynamics. *Earth Planet. Sci. Lett.* **86**, 175–203.
- Allègre C. J. and Turcotte D. L. (1985) Geodynamical mixing in the mesosphere boundary layer and the origin of oceanic islands. *Geophys. Res. Lett.* **12**, 207–210.
- Allègre C. J. and Turcotte D. L. (1986) Implications of a two-component marble-cake mantle. *Nature* **323**, 123–127.
- Allègre C. J. and Lewin E. (1989) Chemical structure and history of the Earth: Evidence from global non-linear inversion of isotopic data in a three box model. *Earth Planet. Sci. Lett.* **96**, 61–88.
- Allègre C. J., Pineau F., Bernat M., and Javoy M. (1971) Evidence for the occurrence of carbonatites on the Cape Verde and Canary Islands. *Nature Phys. Sci.* **233**, 103–104.
- Allègre C. J., Hart S. R., and Minster J. F. (1983) Chemical structure of the mantle and continents determined by inversion of Nd and Sr isotopic data, II. Numerical experiments and discussion. *Earth Planet. Sci. Lett.* **66**, 191–213.
- Allègre C. J., Staudacher T., and Sarda P. (1986) Rare gas systematics: Formation of the atmosphere, evolution and structure of the earth's mantle. *Earth Planet. Sci. Lett.* **81**, 127–150.
- Allègre C. J., Hamelin B., Provost A., and Dupré B. (1986/1987) Topology in isotopic multispace and origin of mantle chemical heterogeneities. *Earth Planet. Sci. Lett.* **81**, 319–337.
- Allègre C. J., Moreira M., and Staudacher T. (1995) $^4\text{He}/^3\text{He}$ dispersion and mantle convection. *Geophys. Res. Lett.* **22**, 2325–2328.
- Beattie P. (1993a) The generation of uranium series disequilibria by partial melting of spinel peridotite: Constraints from partitioning studies. *Earth Planet. Sci. Lett.* **117**, 379–391.
- Beattie P. (1993b) Uranium-thorium disequilibria and partitioning on melting of garnet peridotite. *Nature* **363**, 63–65.
- Breddam K. and Kurz M. D. (2001) Helium isotopic signatures of Icelandic alkaline lavas. *Eos: Trans. Am. Geophys. Union* **82**, 47.
- Cantanzaro E. J., Murphy T. J., Shields W. R., and Garner E. L. (1968) Absolute isotopic abundance ratios of common, equal-Atom, and radiogenic lead isotopic standards. *J. Res. Natl. Bur. Stand.* **72A**, 261–267.
- Chauvel C., Hofmann A. W., and Vidal P. (1992) HIMU-EM: The French Polynesian connection. *Earth Planet. Sci. Lett.* **110**, 99–119.
- Chen C.-Y. and Frey F. A. (1985) Trace element and isotopic geochemistry of lavas from Haleakala Volcano, East Maui, Hawaii; implications for the origin of Hawaiian basalts. *J. Geophys. Res.* **90**, 8743–8768.
- Christensen B. P., Holm P. M., Jambon A., and Wilson J. R. (2001) Helium, argon and lead isotopic composition of volcanics from Santo Antão and Fogo, Cape Verde Islands. *Chem. Geol.* **178**, 127–142.
- Class C. and Goldstein S. L. (1997) Plume-lithosphere interactions in the ocean basins: Constraints from the source mineralogy. *Earth Planet. Sci. Lett.* **150**, 245–260.
- Cliff R. A., Baker P. E., and Mateer N. J. (1991) Geochemistry of Inaccessible Island volcanics. *Earth Planet. Sci. Lett.* **92**, 251–260.
- Cohen R. S. and O'Nions R. K. (1982) Identification of recycled continental material in the mantle from Sr, Nd and Pb isotope investigations. *Earth Planet. Sci. Lett.* **61**, 73–84.
- Condomines M., Grönvold K., Hooker P. J., Muehlen-Bachs K., O'Nions R. K., Oskarsson N., and Oxburgh E. R. (1983) Helium, oxygen, strontium and neodymium isotopic relationships in Icelandic volcanic. *Earth Planet. Sci. Lett.* **66**, 125–136.
- Courtney R. C. and White R. S. (1986) Anomalous heat flow and geoid across the Cape Verde Rise: Evidence for dynamic support from a thermal plume in the mantle. *Geophys. J. R. Astr. Soc.* **87**, 815–867.
- Davaille A. (1999) Simultaneous generation of hotspots and super-swells by convection in a heterogeneous planetary mantle. *Nature* **402**, 756–760.
- Davies G. R., Norry M. J., Gerlach D. C., and Cliff R. A. (1989) A combined chemical and Pb-Sr-Nd isotope study of the Azores and Cape Verde hot-spots: The geodynamic implications. In *Magmatism in the Ocean Basins* (eds. A. D. Saunders and M. J. Norry). *Geol. Soc. Spec. Publ.* **42**, 231–255.
- De Paepe P., Klerkx J., Hertogen J., and Plinke P. (1974) Oceanic tholeiites on the Cape Verde Islands: Petrochemical and geochemical evidence. *Earth Planet. Sci. Lett.* **22**, 347–354.
- Dosso L., Bougault H., and Joron J.-L. (1993) Geochemical morphology of the North Mid-Atlantic Ridge, 10°–20°N: Trace element-isotope complementarity. *Earth Planet. Sci. Lett.* **120**, 443–462.
- Duncan R. A. (1980) Hotspots in the southern ocean—An absolute frame of reference for motion of the Gondwana continents. *Tectonophysics* **74**, 29–42.
- Dupré B., Lambret B., and Allègre C. J. (1982) Isotopic variations within a single island: The Terceira case. *Nature* **299**, 620–622.
- Dupuy C., Barszczus H. G., Liotard J. M., and Dostal J. (1988) Trace element evidence for the origin of oceanic island basalts: An example from the Austral Islands (French Polynesia). *Contrib. Mineral. Petrol.* **98**, 293–302.
- Farnetani C. G., Legras B., and Tackley P. J. (2002) Mixing and deformations in mantle plumes. *Earth Planet. Sci. Lett.* **196**, 1–15.
- Fraser K. J., Hawkesworth C. J., Erlank A. J., Mitchell R. H., and Scott-Smith B. H. (1985/1986) Sr, Nd and Pb isotope and minor element geochemistry of lamproites and kimberlites. *Earth Planet. Sci. Lett.* **76**, 57–70.

- Gautheron C. and Moreira M. (2002) Helium signature of the subcontinental mantle. *Earth Planet. Sci. Lett.* **199**, 39–47.
- Gerlach D. C., Cliff R. A., Davies G. R., Norry M., and Hodgson N. (1988) Magma sources of the Cape Verdes archipelago: Isotopic and trace element constraints. *Geochim. Cosmochim. Acta* **52**, 2979–2992.
- Graham D. W., Humphris S. E., Jenkins W. J., and Kurz M. D. (1992) Helium isotope geochemistry of some volcanic rocks from Saint Helena. *Earth Planet. Sci. Lett.* **110**, 121–131.
- Hart S. R. (1984) A large-scale isotope anomaly in the Southern Hemisphere mantle. *Nature* **309**, 753–757.
- Hart S. R. (1988) Heterogeneous mantle domains: Signatures, genesis and mixing chronology. *Earth Planet. Sci. Lett.* **90**, 273–296.
- Hart S. R. and Zindler A. (1986) In search of a bulk Earth composition. *Chem. Geol.* **57**, 247–267.
- Hanyu T. and Kaneoka I. (1997) The uniform and low $^3\text{He}/^4\text{He}$ ratios of HIMU basalts as evidence for their origin as recycled materials. *Nature* **390**, 273–276.
- Hawkesworth C. J., Kempton P. D., Rogers N. W., Ellam R. M., and van Calsteren P. W. (1990) Continental mantle lithosphere and shallow level enrichment processes in the Earth's mantle. *Earth Planet. Sci. Lett.* **96**, 256–268.
- Hilton D. R., Barling J., and Wheller G. E. (1995) Effects of shallow-level contamination on the helium isotope systematics of ocean-island lavas. *Nature* **373**, 330–333.
- Hoernle K., Tilton G., Le Bas M. J., Duggen S., and Garbe-Schönberg D. (2002) Geochemistry of oceanic carbonatites compared with continental carbonatites: Mantle recycling of oceanic crustal carbonate. *Contrib. Mineral. Petrol.* **142**, 520–542.
- Hofmann A. W. (1988) Chemical differentiation of the Earth: The relationship between mantle, continental crust and oceanic crust. *Earth Planet. Sci. Lett.* **90**, 297–314.
- Hofmann A. W. and White W. M. (1982) Mantle plumes from ancient oceanic crust. *Earth Planet. Sci. Lett.* **57**, 421–436.
- Irving A. J. (1978) A review of experimental studies of crystal/liquid trace element partitioning. *Geochim. Cosmochim. Acta* **42**, 743–770.
- Jagoutz E., Palme H., Baddenhausen H., Blum K., Cendales M., Dreibus G., Spettel B., Lorentz V., and Wänke H. (1979) The abundance of major, minor and trace elements in the Earth's mantle as derived from primitive ultramafic nodules. In *Proc. 10th Lunar Planet. Sci. Conf.* pp. 2031–2050.
- Jørgensen J. Ø. and Holm P. M. (2002) Temporal variation and carbonatite contamination in primitive ocean island volcanics from São Vicente, Cape Verde Islands. *Chem. Geol.* **192**, 249–267.
- Joron J.-L. and Treuil M. (1989) Hygromagmaphile element distributions in oceanic basalts as fingerprints of partial melting and mantle heterogeneities: A specific approach and proposal of an identification and modelling method. In *Magmatism in the Ocean Basins* (eds. A. D. Saunders and M. J. Norry). *Geol. Soc. Spec. Publ.* **42**, 277–299.
- Kelemen P. B., Shimizu N., and Dunn T. (1993) Relative depletion of niobium in some arc magmas and the continental crust: Partitioning of K, Nb, La and Ce during melt/rock interaction in the upper mantle. *Earth Planet. Sci. Lett.* **120**, 111–134.
- Klerkx J. and De Paepe P. (1971) Cape Verde Islands: Evidence for a Mesozoic oceanic ridge. *Nature Phys. Sci.* **233**, 117–118.
- Klerkx J., Deutsch S., and De Paepe P. (1974) Rubidium, strontium content and strontium isotopic composition of strongly alkaline basaltic rocks from the Cape Verde Islands. *Contrib. Mineral. Petrol.* **45**, 107–118.
- Kokfelt T. F., Holm P. M., Hawkesworth C. J., and Peate D. W. (1998) A lithospheric mantle source for the Cape Verde Island magmatism: Trace element and isotopic evidence from the island of Fogo. *Min. Mag.* **62A**, 801–802.
- Kurz M. D. (1986) Cosmogenic helium in a terrestrial igneous rock. *Nature* **320**, 435–439.
- Kurz M. D., Jenkins W. J., Schilling J.-G., and Hart S. R. (1982) Helium isotopic variation in the mantle beneath the central North Atlantic Ocean. *Earth Planet. Sci. Lett.* **58**, 1–14.
- Kurz M. D., Kenn T. C., Lassiter J. C., and DePaolo D. J. (1996) Helium isotopic evolution of Mauna Kea Volcano: First results from the 1 km drill core. *J. Geophys. Res.* **101**, 11781–11791.
- Langmuir C. H., Vocke R. D., Hanson G. N., and Hart S. R. (1978) A general mixing equation with applications to Icelandic basalts. *Earth Planet. Sci. Lett.* **37**, 380–392.
- Lassiter J. C., Hauri E. H., Reiners P. W., and Garcia M. O. (2000) Generation of Hawaiian post-erosional lavas by melting of a mixed lherzolite/pyroxenite source. *Earth Planet. Sci. Lett.* **178**, 269–284.
- La Tourette T. Z., Hervig R. L., and Holloway J. R. (1995) Trace element partitioning between amphibole, phlogopite and basanite melt. *Earth Planet. Sci. Lett.* **135**, 13–30.
- Le Pichon X. and Fox P. J. (1971) Marginal offsets, fractures zones and the early opening of the North Atlantic. *J. Geophys. Res.* **76**, 6294–6308.
- Le Roex A. P., Cliff R. A., and Adair B. J. I. (1990) Tristan da Cunha, South Atlantic: Geochemistry and petrogenesis of a basanite-phonolite lava series. *J. Petrol.* **31**, 779–812.
- Manhès G., Minster J.-F., and Allègre C. J. (1978) Comparative U-Th-Pb and Rb-Sr study of the St. Severin amphoterites: Consequence for early solar system chronology. *Earth Planet. Sci. Lett.* **39**, 14–24.
- Matos Alves C. A., Macedo J. R., Silva L. C., Serralheiro A., and Peixoto A. F. (1979) Estudo geológico, petrológico e vulcanológico da Ilha de Santiago (Cabo Verde). *Garcia de Orta Sér. Geol. Lisboa* **3**, 47–74.
- McDonough W. F. and Sun S. S. (1995) The composition of the Earth. *Chem. Geol.* **120**, 223–253.
- McKenzie D. and O'Nions R. K. (1983) Mantle reservoirs and ocean island basalts. *Nature* **301**, 229–231.
- Mendes M. H. and Silva L. C. (2001) Xenólitos crustais nas ilhas de Cabo Verde: Características petrográficas e química mineral. In *VI Congresso de Geoquímica dos Países de Língua Portuguesa, Universidade do Algarve, Faro*, pp. 153–156.
- Moreira M. and Kurz M. D. (2001) Subducted oceanic lithosphere and the origin of the “high μ ” basalt helium isotopic signature. *Earth Planet. Sci. Lett.* **189**, 49–57.
- Moreira M., Doucelance R., Kurz M. D., Dupré B., and Allègre C. J. (1999) Helium and lead isotope geochemistry of the Azores Archipelago. *Earth Planet. Sci. Lett.* **169**, 189–205.
- Paster T. P., Schauwecker D. S., and Haskin L. A. (1974) The behaviour of some trace elements during solidification of the Skaergaard layered series. *Geochim. Cosmochim. Acta* **38**, 1549–1577.
- Pin C. and Bassin C. (1992) Evaluation of a strontium-specific extraction chromatographic method for isotopic analysis in geological materials. *Anal. Chim. Acta* **269**, 249–255.
- Rollinson H. (1993) *Using Geochemical Data: Evaluation, Presentation, Interpretation*. Longman Scientific & Technical, Essex, UK.
- Serralheiro A. (1976) A geologia da ilha de Santiago. *Bol. Mus. Lab. Min. Geol. Fac. Ciênc. Lisboa* **14**, 2, 218.
- Thirlwall M. F. (1997) Pb isotopic and elemental evidence for OIB derivation from young HIMU mantle. *Chem. Geol.* **139**, 51–74.
- Thirlwall M. F. (2001) Inappropriate tail corrections can cause large inaccuracy in isotope ratio analysis by MC-ICP-MS. *J. Anal. At. Spectrom.* **16**, 1121–1125.
- Thirlwall M. F. (2002) Multicollector ICP-MS analysis of Pb isotopes using a ^{207}Pb - ^{204}Pb double spike demonstrates up to 400 ppm/amu systematic errors in Tl-normalization. *Chem. Geol.* **184**, 255–279.
- Trindade M. J., Munha J., and Mata J. (2001) Geoquímica das “lavas recentes” da ilha de S. Vicente (Cabo Verde): Evidências para a existência de heterogeneidades mantélicas verticais e horizontais. In *VI Congresso de Geoquímica dos Países de Língua Portuguesa, Universidade do Algarve, Faro*, pp. 197–200.
- Turcotte D. L. and Schubert G. (1982) From direct integration of Table F, Appendix 2. In *Geodynamics: Applications of Continuum Physics to Geological Problems*, pp. 432–433. John Wiley, New York.
- Turner S., Hawkesworth C., Rogers N., and King P. (1997) U-Th isotope disequilibria and ocean island basalt generation in the Azores. *Chem. Geol.* **139**, 145–164.
- Vollmer R. (1983) Earth degassing, mantle metasomatism and isotopic evolution of the mantle. *Geology* **11**, 452–454.
- Weaver B. L. (1991) The origin of ocean island basalt end-member compositions: Trace element and isotopic constraints. *Earth Planet. Sci. Lett.* **104**, 381–397.
- White W. M. (1985) Sources of oceanic basalts: radiogenic isotopic evidence. *Geology* **13**, 115–118.

- Woodhead J. D. (1996) Extreme HIMU in an oceanic setting: The geochemistry of Mangaia Island (Polynesia), and temporal evolution of the Cook-Austral hotspot. *J. Volcanol. Geotherm. Res.* **72**, 1–19.
- Zartman R. E. and Haines S. M. (1988) The plumbotectonic model for Pb isotopic systematics among major terrestrial reservoirs—A case for bi-directional transport. *Geochim. Cosmochim. Acta* **52**, 1327–1339.
- Zindler A. and Hart S. R. (1986a) Chemical geodynamics. *Ann. Rev. Earth Planet. Sci.* **14**, 493–571.
- Zindler A. and Hart S. R. (1986b) Helium: Problematic primordial signals. *Earth Planet. Sci. Lett.* **79**, 1–8.
- Zindler A., Jagoutz E., and Goldstein S. L. (1982) Nd, Sr and Pb isotopic systematics in a three-component mantle: A new perspective. *Nature* **298**, 519–523.

APPENDIX

Sr and Pb Isotopic Composition of the Lower Mantle

Complementarity between the continental crust (CC) and the depleted mantle (DM), with respect to the Bulk Silicate Earth (BE), is assumed. Following Allègre and Lewin (1989) the mass balance equations for isotopic pairs (radiogenic element X) and absolute concentrations (reference stable isotope ^SX) are

$$\alpha_{\text{BE}}^{\text{X}} = \alpha_{\text{CC}}^{\text{X}} \cdot W^{\text{X}} + \alpha_{\text{DM}}^{\text{X}} \cdot (1 - W^{\text{X}}) \quad (\text{A1})$$

$$[^S\text{X}]_{\text{BE}} = \phi \cdot [^S\text{X}]_{\text{CC}} + (1 - \phi) \cdot [^S\text{X}]_{\text{DM}} \quad (\text{A2})$$

where α refers to the isotopic ratio, W^{X} to the sialic index, which indicates the preferential affinity of an element for the continental crust (cf. Allègre and Lewin, 1989), and ϕ to the mass fraction of continental crust, using the value of Allègre and Lewin (1989) i.e., $\phi = 0.015$;

$$W^{\text{X}} = \phi \cdot [^S\text{X}]_{\text{CC}} / [^S\text{X}]_{\text{BE}} \quad (\text{A3})$$

$$\phi = \text{mass}_{\text{CC}} / (\text{mass}_{\text{DM}} + \text{mass}_{\text{CC}}) \quad (\text{A4})$$

where mass_{DM} is the mass of depleted mantle and mass_{CC} that of the continental crust.

Combination of Eqn. A1 to A4 yields the chemical ratio $[^S\text{X}]_{\text{DM}} / [^S\text{X}]_{\text{BE}}$. Since depletion affects a portion of the mantle that is greater than the upper mantle alone (Jagoutz et al., 1979; Allègre et al., 1983; Hart and Zindler, 1986), the lower mantle (LM) composition is represented by a mixture of depleted and Bulk Silicate Earth materials. Since oceanic crust and sediments potentially recycled into the lower mantle through subduction mainly sink at the base (D'' layer), the mass of recycled material into the lower mantle is considered negligible. In this model, mass balance equations for isotopic pairs and absolute concentrations are

$$\alpha_{\text{LM}}^{\text{X}} = \alpha_{\text{BE}}^{\text{X}} \cdot U^{\text{X}} + \alpha_{\text{DM}}^{\text{X}} \cdot (1 - U^{\text{X}}) \quad (\text{A5})$$

$$[^S\text{X}]_{\text{LM}} = f \cdot [^S\text{X}]_{\text{DM}} + (1 - f) \cdot [^S\text{X}]_{\text{BE}} \quad (\text{A6})$$

where U^{X} is the proportion of BE material and f the fraction of depleted mantle in the lower mantle. Then

$$U^{\text{X}} = (1 - f) \cdot [^S\text{X}]_{\text{BE}} / [^S\text{X}]_{\text{LM}} \quad (\text{A7})$$

$$f = (\text{mass}_{\text{DM}} - \text{mass}_{\text{UM}}) / \text{mass}_{\text{LM}} = (\text{mass}_{\text{DM}} - \text{mass}_{\text{UM}}) / (\text{mass}_{\text{MM}} - \text{mass}_{\text{UM}}) \quad (\text{A8})$$

where mass_{UM} is the mass of the upper mantle and mass_{MM} the total mass of the mantle.

Eqn. A6 yields the chemical ratio $[^S\text{X}]_{\text{LM}} / [^S\text{X}]_{\text{BE}}$; combining Eqn. A5 and A7 leads to the isotopic composition of the lower mantle. Given that $\text{mass}_{\text{UM}} / \text{mass}_{\text{MM}} = 25.6\%$ (Turcotte and Schubert, 1982) and $\text{mass}_{\text{DM}} / \text{mass}_{\text{MM}} = 38.1\%$ (Allègre and Lewin, 1989), $f = 16.8\%$.